

# The Solubility of Gases in Ionic Liquids

**Mark B. Shiflett**

Chemical and Petroleum Engineering, Center for Environmentally Beneficial Catalysis, University of Kansas, Lawrence, KS 66047

**Edward J. Maginn**

Chemical and Biomolecular Engineering, University of Notre Dame, Notre Dame, IN 46556

DOI 10.1002/aic.15957

Published online September 21, 2017 in Wiley Online Library (wileyonlinelibrary.com)

*In this Perspective, we provide a detailed discussion of the techniques and methods used for determining the solubility of gases in ionic liquids (ILs). This includes various experimental measurement techniques, equation of state (EOS) modeling, and predictive molecular-based modeling. Many of the key papers from the past 15 years are discussed and put into the context of the latest advances in the field. Limitations of these methods plus future developments and new research opportunities are discussed. © 2017 American Institute of Chemical Engineers AIChE J, 63: 4722–4737, 2017*  
**Keywords:** ionic liquids, gas solubility, absorption, phase equilibria, isotherm, modeling

## History of ILs

The first observations of materials we now recognize as ILs are believed to date back as far as the mid-nineteenth century, when Friedel and Crafts described the formation of a “red oil,” which often appeared in their alkylation and acylation reactions.<sup>1,2</sup> The red oil, which was identified almost a century later by chemists in Japan, consisted of an alkylated aromatic ring cation and a chloroaluminate anion, which by definition was an IL.<sup>1,3</sup> Paul Walden in 1914 is credited with publishing the first scientific paper that described the synthesis of the room-temperature IL ethylammonium nitrate, which has a melting point of 12.5°C.<sup>4</sup> However, it was not until 1992 when John Wilkes and Michael Zaworotko at the U.S. Air Force Academy reported the synthesis of the first “air and water stable” imidazolium ILs, such as 1-ethyl-3-methylimidazolium hexafluorophosphate and 1-ethyl-3-methylimidazolium tetrafluoroborate, that the field began to expand.<sup>5</sup> Wilkes later wrote one of the first review papers on ILs entitled “A short history of ionic liquids – from molten salts to neoteric solvents.”<sup>6</sup>

In April 2000, the first NATO advanced research workshop (ARW) on ILs was held in Heraklion, Crete. The conference was the first international meeting devoted to ILs and attracted most of the active researchers at that time. Following that meeting, activity in the field began to flourish and the first books and international conferences devoted to ILs began to appear.

The first book dedicated to ILs was edited by Kenneth Seddon and Robin Rogers in 2002 entitled “Ionic Liquids, Industrial Applications to Green Chemistry.”<sup>7</sup> This book contained the key papers from the American Chemical Society National Meeting

symposium, “Green (or Greener) Industrial Applications of Ionic Liquids” held in San Diego, California, April 1–5, 2001. The symposium was the first “open” international meeting on the fundamentals and applications of ILs (the NATO ARW meeting held in Crete was by invitation). Another seminal text that appeared in 2002 edited by Peter Wasserscheid and Tom Welton was entitled “Ionic Liquids in Synthesis.”<sup>8</sup> The book was designed to take the reader from little or no knowledge of ILs to an understanding reflecting the best knowledge at that time. These authors are now eminent scholars in the field of ILs.

A number of other excellent books have been written about ILs, some which now specialize in particular fields of use such as organic synthesis, electrochemistry, bio-processing, pharmaceuticals, catalysis, separations, and industrial applications.<sup>1,9–36</sup> The field has rapidly expanded, and a recent Scifinder and Web of Science search using the key word “ionic liquid” estimates that over 20,000 publications and 4,000 patents have been published since 2012 (i.e., over 100 references per week for the past 5 years).

The solubility of gases has played an important role in the history of ILs, which traditionally have been considered as new solvents for both separations and chemical reactions.<sup>7–36</sup> In gas separations, the design of the absorption (desorption) column requires solubility data for the gases in the ILs. In gas–liquid reactions such as alkylation, hydrogenation, and hydroformylation, the mass transfer of the gas in the IL phase is needed to design the chemical reactor. Other applications which require knowledge of gas solubility in ILs include absorption cooling, polymerization, membranes, lubrication, extraction, and gas-expanded liquids to name a few.

## Gas Solubility in ILs

ILs are defined as molten salts with a melting temperature below about 373 K.<sup>8,15,16</sup> ILs have received significant attention

Correspondence concerning this article should be addressed to M. B. Shiflett at Mark.B.Shiflett@ku.edu

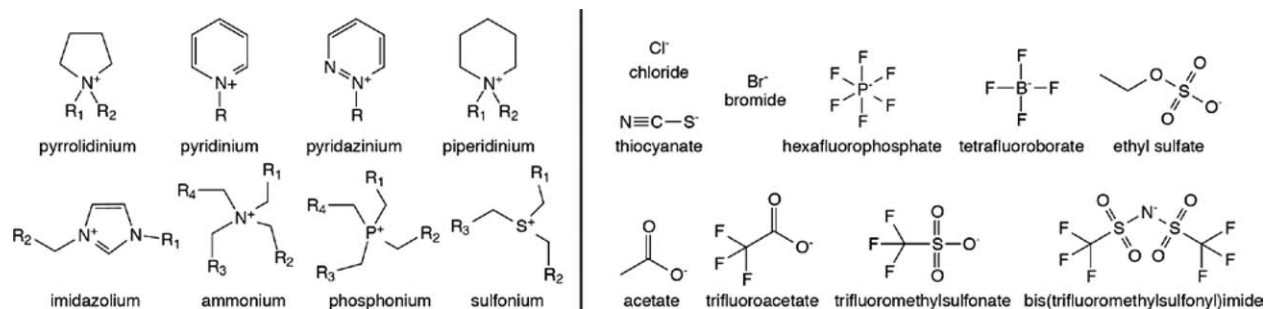


Figure 1. Chemical structure for common cations and anions.

due to their low vapor pressure, high chemical and thermal stability, and the large variety of cations and anions that can be synthesized.<sup>8,15,16</sup> Figure 1 provides the structures for some of the most common cations and anions.

A variety of thermophysical property data have been published for ILs. The NIST Ionic Liquids Database (ILThermo v2.0)<sup>37,38</sup> is a free web research tool that allows users worldwide to access an up-to-date data collection from publications on experimental studies of thermodynamic and transport properties of ILs. The database contains gas solubility data as well as information on chemical identification, sample purity, phase transitions, transport, volumetric and thermal properties, surface tension, refractive index, speed of sound, vapor pressure, and activity coefficients with details of experimental methods and numerical data uncertainty.

A recent literature search found over 200 references published in the past 5 years (2012–2017) on the “solubility of gases in ionic liquids,” and a recent review by Lei et al. in 2014 provides the solubility for several gases ( $H_2$ ,  $O_2$ ,  $N_2$ ,  $CO$ ,  $CO_2$ ,  $Ar$ ,  $Xe$ ,  $Kr$ ,  $SO_2$ ,  $H_2S$ ,  $N_2O$ ,  $NO_2$ ,  $NH_3$ ,  $H_2O$ , hydrocarbons, and hydrofluorocarbons) in a variety of ILs with over 350 references.<sup>39</sup> The results are often reported as the Henry’s Law constant; however, we believe that the description of gas solubility in ILs should include the global phase behavior (i.e., vapor–liquid equilibria [VLE], vapor–liquid–liquid equilibria [VLLE], and liquid–liquid equilibria [LLE]).<sup>40,41</sup>

The main focus of this Perspective is to emphasize the importance of characterizing the complete phase behavior (i.e., gas mole fraction from  $0 \leq x \leq 1$ ) over a wide temperature and pressure range and utilizing simulation tools to understand the molecular interactions. Several gas + IL systems exhibit both miscible (VLE) and immiscible regions (VLLE and LLE) that can be classified according to the type of high-pressure phase behavior defined by van Konynenburg and Scott.<sup>42,43</sup> To understand such a wide range of phase behavior, EOS methods are required and one will be briefly described.

Initially, we had some doubt about whether a nonelectrolyte EOS could work for IL mixtures; however, the EOS method works well for  $PVT_x$  phase calculations. This should not be surprising, because the thermodynamic equilibrium for VLE does not depend on knowing the structure of the liquid. Here, molecular simulations can provide a detailed understanding of the gas + IL interactions.

## VLE Measurements

To accurately measure the solubility of a gas in an IL requires: (i) purification and characterization of the solute gas and IL; (ii) thorough drying and degassing of the IL; (iii) equilibration of the gas and IL phases under the conditions of known constant temperature and pressure; (iv) measurements that determine the composition of the gas in the IL phase; (v) proper error analysis to estimate the uncertainty; and (vi) use of a thermodynamic model to validate results.<sup>41</sup> Any paper reporting data on the solubility of a gas in a IL should include an adequate description of these steps and comparison measurements on a standard system to allow the user to judge the reliability of the data.<sup>44</sup> For this purpose, the International Union of Pure and Applied Chemistry (IUPAC) sponsored a project to make physical property measurements available for comparing the gas solubility of  $CO_2$  in a reference IL, 1-hexyl-3-methylimidazolium bis(trifluoromethylsulfonyl)imide (commonly abbreviated [hmim][Tf<sub>2</sub>N], [C<sub>6</sub>mim][NTf<sub>2</sub>], or [C<sub>6</sub>C<sub>1</sub>im][Tf<sub>2</sub>N]).<sup>45,46</sup> The report provides both recommended gas absorption methods and reference values for VLE and LLE of  $CO_2$  in [C<sub>6</sub>C<sub>1</sub>im][Tf<sub>2</sub>N].<sup>46</sup>

A variety of experimental methods have been used to measure the solubility of gases in ILs including physical methods (gravimetric and synthetic) and analytical methods (chromatographic and spectroscopic).

### Gravimetric method

A common technique used to measure the solubility of gases in ILs is the gravimetric method. Although this method was originally developed to measure gas adsorption on solids such as zeolites and carbons, it can be applied to ILs because their extremely low vapor pressure prevents evaporation of the sample. This technique was used by Maginn and Brennecke who published some of the first papers on the solubility of gases in ILs.<sup>47–49</sup> The advantages of a microbalance include the minimal sample size required (<100 mg IL), the ability to measure both gas solubility and diffusivity simultaneously,<sup>50</sup> and the flexibility to acquire absorption and desorption isotherms. Figure 2 provides a schematic of a Hiden gravimetric microbalance (XEMIS).<sup>51</sup>

### Synthetic methods

Several variations of the synthetic (or stoichiometric) method exist, which involve adding a precise amount of gas and IL into a high-pressure view cell with a known volume.

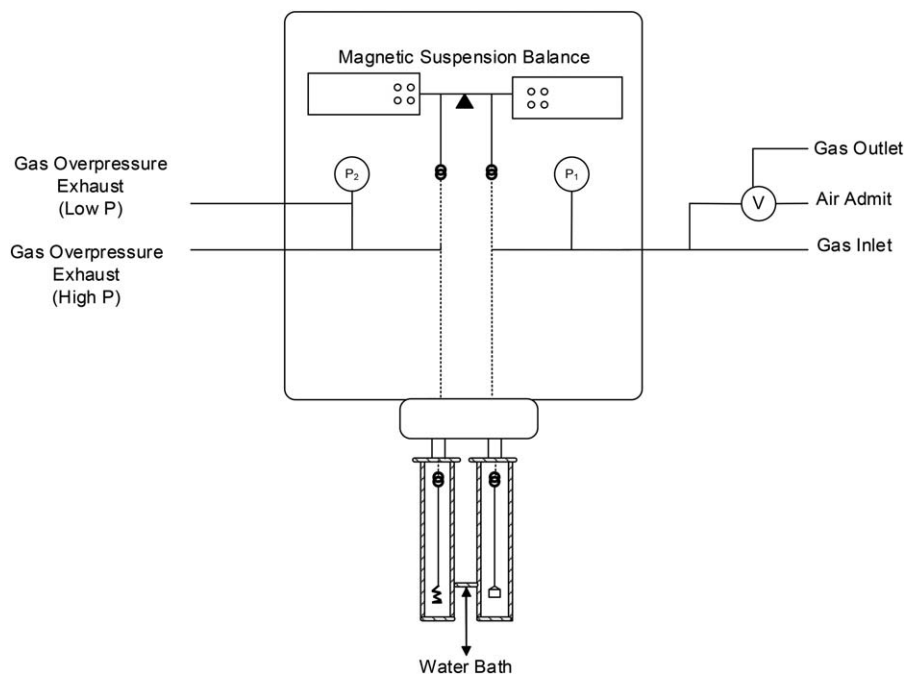


Figure 2. Schematic diagram of Hidden Isochema XEMIS gravimetric microbalance.<sup>54</sup>

One method used by several researchers involves increasing the pressure (at constant temperature) until all the gas dissolves in the IL and the last bubble disappears (bubble point method).<sup>52–60</sup> A variation of this method involves continuing continuously increasing the pressure using a variable-volume view cell and then slowly decreasing the pressure until the first bubble appears.<sup>61</sup> Maurer and coworkers have used a similar method, but observe the phase change by adding and withdrawing known amounts of the IL to pressurize (depressurize) the mixture.<sup>62–65</sup> The method developed by Ren and Scurto measures the vapor and liquid phase volumes and calculates the solubility, molar volume, volume expansion, and density of the liquid solution.<sup>66–68</sup>

A pressure drop method is also used with a calibrated gas volume ( $V_1$ ) at a given  $T$  and  $P$ . A known amount of IL is added to a second calibrated volume ( $V_2$ ) which is connected by a valve to  $V_1$ . When the valve is opened the gas fills both volumes and dissolves in the IL. Measurement of the pressure drop at equilibrium allows the number of moles of gas to be calculated in the vapor and liquid phase (by difference). This technique has been used by Costa Gomes and coworkers in glassware at low pressures and is ideal for measuring dilute solutions to obtain Henry's Law constants.<sup>69–73</sup>

### Chromatographic methods

Gas chromatography (GC) has been used to measure infinite dilution activity coefficients and the equivalent Henry's Law constants. A chromatography column is coated with an IL and the solute (gas or liquid) is introduced with a carrier gas. The retention time of the solute is measured at steady state, and the strength of the interaction of the solute in the IL determines the infinite dilution activity coefficient. This technique has been used by Heintz et al. to measure the infinite dilution activity coefficients of liquids in ILs.<sup>74–76</sup>

### Spectroscopic methods

Infrared and  $^1\text{H-NMR}$  spectroscopy has been used to measure the solubility of gases in ILs. Welton and coworkers used ATR-IR and  $^1\text{H-NMR}$  to measure the solubility of carbon dioxide and hydrogen in ILs, respectively.<sup>77</sup> UV-vis absorption, Raman,  $^1\text{H-NMR}$  and  $^{13}\text{C-NMR}$  spectroscopy have been used to characterize the interactions between gases and ILs.<sup>78</sup>

### LLE Measurements

LLE measurements have been successfully conducted using a simple mass-volume technique.<sup>79,80</sup> When a binary system exhibits a liquid-liquid separation (or VLLE), it is an *univariant* state according to the Gibbs phase rule. This means that at a given intensive variable, for example, temperature, there is no freedom for other intensive variables. All other variables such as compositions, pressure, and densities of the system are uniquely determined regardless of any different extensive variables (volume of each phase and total mass of the system). The overall feed composition merely changes the physical volume in each phase, but the composition and density in each phase remains constant as long as the three phases exist at the fixed  $T$ .

This unique VLLE state of a binary system can be determined experimentally using a simple apparatus by mass and volume measurements *alone* without using any analytical method for the composition analysis. A set of mass and volume measurements of two sample containers at a constant temperature is sufficient to determine the required thermodynamic properties.<sup>79,80</sup>

Mixing time to reach equilibrium can take several hours to days and is one of the most critical properties for properly measuring VLLE whether using this method or the more common cloud-point method.<sup>81–86</sup> The time required to effectively

mix the gas + IL systems and reach equilibrium depends on the choice of IL, the gas and the solution viscosity.

## Modeling Gas Solubility

Measuring and reporting the solubility of a gas in an IL does not ensure that the results are thermodynamically consistent. A thermodynamic model should be applied to check the data quality and can be useful in making predictions. The thermodynamic phase behaviors of gases with ILs can be well modeled with activity models and EOS methods.<sup>87,88</sup>

Several activity models are available in the literature<sup>89–91</sup> and the experimental ( $PTx$ ) results have been analyzed using the nonrandom two liquid model.<sup>92–94</sup> However, activity models (or any solution models) are inaccurate (or undefined) at high temperatures, particularly near and above the  $T_c$  of the gaseous species. Therefore, extrapolations for phase behaviors over wide  $T$  and  $P$  ranges must be treated with caution. Also, the prediction of LLE based only on VLE data, or vice versa, is not numerically accurate with any conventional activity model.<sup>90</sup> More reliable predictions of the global phase behavior can be made using an EOS.

### EOS modeling

A variety of EOS models have been reported<sup>39</sup> to describe phase behavior of gases in ILs such as the generic Redlich–Kwong (RK) type of cubic EOS<sup>95,96</sup>

$$P = \frac{RT}{V-b} - \frac{a(T)}{V(V+b)} \quad (1)$$

$$a(T) = 0.427480 \frac{R^2 T_c^2}{P_c} \alpha(T) \quad (2)$$

$$b = 0.08664 \frac{RT_c}{P_c}, \quad (R : \text{universal gas constant}) \quad (3)$$

The temperature-dependent part of the ( $a$ ) parameter in the EOS for pure compounds is modeled by the following empirical equations<sup>96</sup>

$$\alpha(T) = \sum_{k=0}^{\leq 3} \beta_k (1/T_r - T_r)^k, \quad \text{for } T_r \equiv T/T_c \leq 1 \quad (4a)$$

$$\alpha(T) = \beta_0 + \beta_1 [\exp \{2(1-T_r)\} - 1], \quad \text{for } T_r \geq 1 \quad (4b)$$

The coefficients,  $\beta_k$ , are determined so as to reproduce the vapor pressure of each pure compound. It should be noted that Eq. 4b is implemented for  $T_r \geq 1$  in order for  $\alpha(T)$  to be physically meaningful for gases even at very high temperatures. Equation 4b is always  $\alpha(T) > 0$  and a decreasing function with  $T$ . When  $T_r = 1$ , Eqs. 4a and 4b are set to be analytically continuous.

Typically for ILs, no vapor pressure data are available because they are practically nonvolatile. Also, estimated data for the critical parameters ( $T_c$  and  $P_c$ ) exist<sup>97–102</sup>; however, only rough estimates are required for the present EOS modeling. The  $T_c$  are hypothetical values because they are above the decomposition  $T$  for ILs. On the other hand, the temperature-dependent part of the  $a$  parameter of ILs (Eq. 2) is significant when trying to correlate the solubility (pressure-temperature-composition:  $PTx$ ) data, despite the vapor pressure of ILs being essentially zero at the temperature of interest. Therefore,

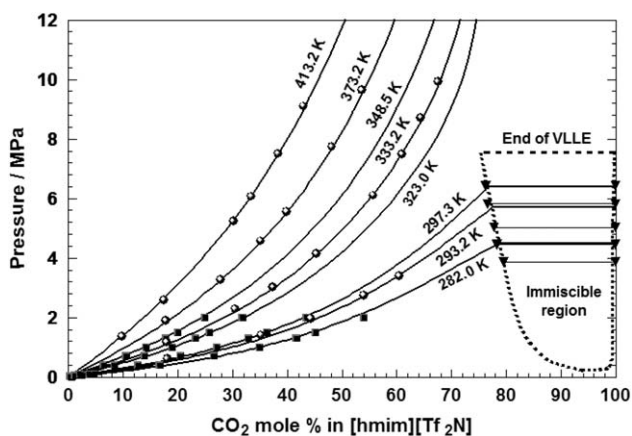


**Figure 3.** Isothermal  $P_x$  phase diagram for  $\text{CO}_2 + [\text{hmim}][\text{Tf}_2\text{N}]$  (i.e.,  $[\text{C}_6\text{C}_1\text{im}][\text{Tf}_2\text{N}]$ ).

Solid lines: calculated using the EOS model.<sup>87</sup> Symbols: ●, VLE data<sup>64</sup>; ■, VLE data<sup>87</sup>; ▼, VLLE data<sup>87</sup>; figure was used with permission.<sup>87</sup>

the coefficient  $\beta_1$  for ILs in Eq. 4 is usually treated as an adjustable fitting parameter using  $\beta_0 = 1$  and  $\beta_2 = \beta_3 = 0$  in the solubility data analysis, together with the binary interaction parameters discussed below. However, once  $\beta_1$  is determined for a particular IL using a certain binary system, it is used as a fixed constant for any other binary systems containing that IL.

The  $a$  and  $b$  parameters for a general  $N$ -component mixture are modeled in terms of binary interaction parameters<sup>95</sup>

$$a = \sum_{ij=1}^N \sqrt{a_i a_j} f_{ij}(T) (1 - k_{ij}) x_i x_j, \quad a_i = 0.427480 \frac{R^2 T_{ci}^2}{P_{ci}} \alpha_i(T) \quad (5)$$

$$f_{ij}(T) = 1 + \tau_{ij}/T, \quad \text{where } \tau_{ij} = \tau_{ji}, \quad \text{and } \tau_{ii} = 0 \quad (6)$$

$$k_{ij} = \frac{l_{ij} l_{ji} (x_i + x_j)}{l_{ji} x_i + l_{ij} x_j}, \quad \text{where } k_{ii} = 0 \quad (7)$$

$$b = \frac{1}{2} \sum_{ij=1}^N (b_i + b_j) (1 - k_{ij}) (1 - m_{ij}) x_i x_j, \quad b_i = 0.08664 \frac{RT_{ci}}{P_{ci}} \quad (8)$$

where  $m_{ij} = m_{ji}$ , and  $m_{ii} = 0$ ;  $T_{ci}$ , critical temperature of  $i$ th species;  $P_{ci}$ , critical pressure of  $i$ th species; and  $x_i$ , mole fraction of  $i$ th species.

The present EOS model has been successfully applied to a variety of gas + IL systems.<sup>40,41,87,88</sup> Figure 3 provides a comparison of experimental  $PTx$  data ( $\text{CO}_2 + [\text{C}_6\text{C}_1\text{im}][\text{Tf}_2\text{N}]$ ) from the IUPAC project fitted with the RK EOS model.<sup>87</sup> The standard deviation for the  $P$  versus  $x_1$  fit is excellent ( $\pm 0.03$  MPa). The EOS model also predicts a partial immiscibility in  $\text{CO}_2$ -rich solution which has been confirmed using the mass-volume technique to measure LLE behavior as shown in Figure 3. The  $\text{CO}_2 + [\text{C}_6\text{C}_1\text{im}][\text{Tf}_2\text{N}]$  system likely exhibits the Type-III mixture behavior according to the classification of van Konynenburg and Scott.<sup>42,43</sup> In this case, the LLE will intersect with the solid-liquid equilibria such that no lower critical solution temperature (LCST) can exist. In other systems containing hydrofluorocarbons in ILs ( $\text{CHF}_3 + 1\text{-butyl-3-methylimidazolium hexafluorophosphate } \{[\text{C}_4\text{C}_1\text{im}][\text{PF}_6]\}$ ,  $\text{CH}_2\text{FCF}_3 +$

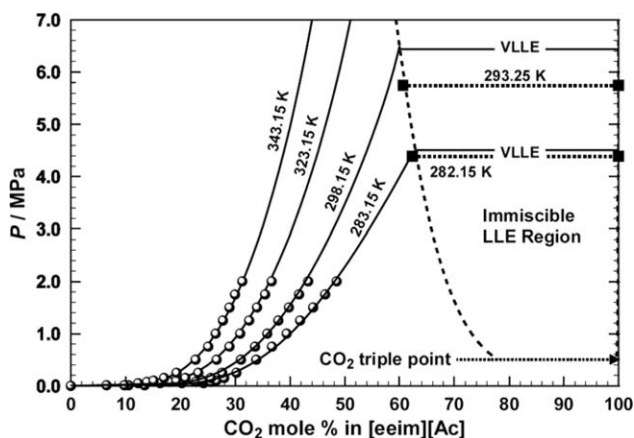


**Figure 4.** Isothermal  $P_x$  phase diagram for  $\text{CO}_2 + [\text{eem}][\text{Ac}]$  (i.e.,  $[\text{C}_2\text{C}_2\text{im}][\text{C}_1\text{CO}_2]$ ).

Solid lines: calculated using the EOS model.<sup>105</sup> Symbols: ●, VLE data<sup>105</sup>; ■, VLLE data<sup>105</sup>; figure was used with permission.<sup>105</sup>

$[\text{C}_4\text{C}_1\text{im}][\text{PF}_6]$ ,  $\text{CH}_3\text{CHF}_2 + [\text{C}_4\text{C}_1\text{im}][\text{PF}_6]$ ,  $\text{CH}_3\text{CH}_2\text{F} + [\text{C}_4\text{C}_1\text{im}][\text{PF}_6]$ , the existence of a LCST supports the Type-V mixture behavior.<sup>80,88</sup> Pure component EOS constants, optimal binary interaction parameters ( $l_{ij}$ ,  $l_{ji}$ ,  $m_{ij}$ , and  $\tau_{ij}$ ), fugacity coefficient, and other derived thermodynamic properties for the  $\text{CO}_2 + [\text{C}_6\text{mim}][\text{Tf}_2\text{N}]$  system are provided in Ref. 87.

Carbon dioxide possesses relatively high solubility in ILs; however, most cases are for physical-type absorption.<sup>41,49,51–55,57–61,63,66,68–72,77,87</sup> Other cases exist such as with  $\text{CO}_2$  and ILs containing an acetate anion (e.g., 1-butyl-3-methylimidazolium acetate  $[\text{C}_4\text{C}_1\text{im}][\text{C}_1\text{CO}_2]$ , 1-ethyl-3-methylimidazolium acetate  $[\text{C}_2\text{C}_1\text{im}][\text{C}_1\text{CO}_2]$  and 1-ethyl-3-ethylimidazolium acetate  $[\text{C}_2\text{C}_2\text{im}][\text{C}_1\text{CO}_2]$ ) where highly negative deviations from Raoult's law indicate chemical absorption instead of ordinary physical absorption.<sup>103–105</sup> As shown in Figure 4, the negative deviation is so large that the pressure of  $\text{CO}_2$  gas becomes practically zero at  $\text{CO}_2$  mole fraction range of less than about 0.3 (30 mole %).<sup>105</sup> The proposed mechanism shown in Figure 5 has been confirmed experimentally by several research groups.<sup>103–108</sup>

To understand the physical meaning of such highly non-ideal phase behavior consider the following two types of chemical absorption behavior for species A and B in a liquid solution<sup>109–114</sup>

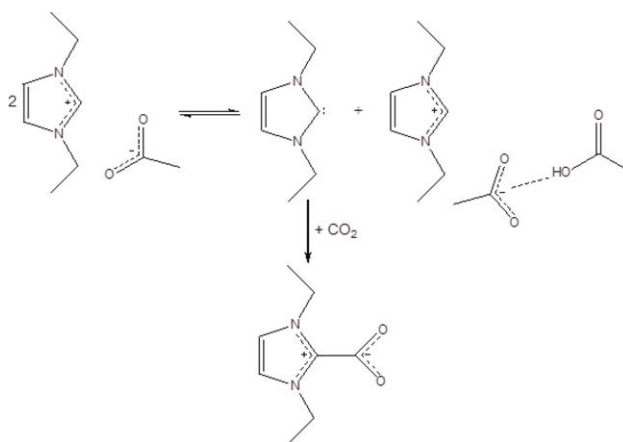


Therefore, in solution, there can exist four species: A, B, AB, and  $\text{AB}_2$ . If we assume that these species form an *ideal solution*, then the following thermodynamic excess functions can be derived<sup>109–114</sup>

$$\frac{G^E}{RT} = (1-x_B) \ln \frac{1-z_B}{(1-x_B)(1+K_1z_B+K_2z_B^2)} + x_B \ln \frac{z_B}{x_B} \quad (11)$$

$$\frac{H^E}{RT} = \frac{(1-x_B)z_B(K_1\Delta H_1 + K_2\Delta H_2z_B)}{RT(1+K_1z_B+K_2z_B^2)} \quad (12)$$

where  $x_B$  = the stoichiometric (or feed) mole fraction of species B,  $z_B$  = the true (or actually existing) mole fraction of B



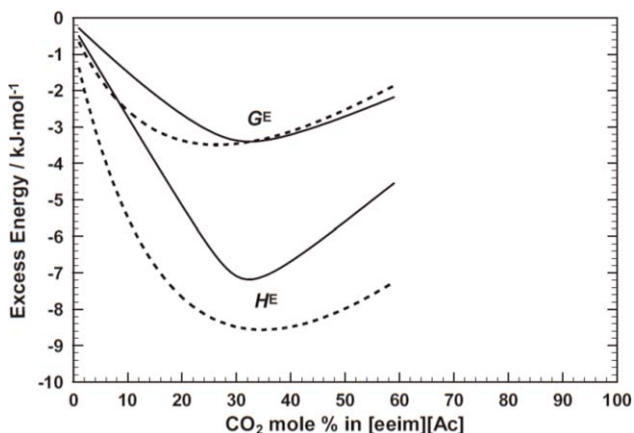
**Figure 5.** Proposed reaction mechanism for  $\text{CO}_2 + [\text{eem}][\text{Ac}]$  (i.e.,  $[\text{C}_2\text{C}_2\text{im}][\text{C}_1\text{CO}_2]$ ).<sup>105–108</sup>

Figure was used with permission.<sup>105–108</sup>

in the solution, and  $\Delta H_1$  and  $\Delta H_2$  are the heats of complex formation for the association reactions of Eqs. 9 and 10, respectively.  $x_B$  is related to  $z_B$  by<sup>109,110</sup>

$$x_B = \frac{(1+K_1)z_B + K_2z_B^2(1-z_B)}{1 + K_1z_B(2-z_B) + K_2z_B^2(3-2z_B)} \quad (13)$$

Using the present EOS, the excess functions,  $G^E$  and  $H^E$ , can be calculated at given  $T$ ,  $P$ , and compositions (see Eqs. S29, S31, and S32 in supporting information of Ref. 105). Species A is designated as  $\text{CO}_2$  and B as the IL. The temperature is taken as 298.15 K, and  $P = 6.5$  MPa, which is close to the vapor pressure of  $\text{CO}_2$  at 298.15 K. Then,  $G^E$  and  $H^E$  from the EOS correlation can be calculated as a function of  $x_A$  ( $=1-x_B$ ) as shown in Figure 6.<sup>105</sup> Also,  $G^E$  and  $H^E$  from the association model can be evaluated similarly as a function of  $x_B$  ( $=1-x_A$ ) with four unknown parameters  $K_1$ ,  $K_2$ ,  $\Delta H_1$ , and  $\Delta H_2$ ; see Eqs. 11–13. These unknown parameters are determined by minimizing the differences of both  $G^E$  and  $H^E$  functions between the EOS and the association models using a



**Figure 6.** Analysis of the ideal association model using an example of  $\text{CO}_2 + [\text{eem}][\text{Ac}]$  (i.e.,  $[\text{C}_2\text{C}_2\text{im}][\text{C}_1\text{CO}_2]$ ).

Solid lines: the EOS model calculation. Dotted lines: results from the association model with the least-squares analysis of  $G^E$  and  $H^E$ ; figure was used with permission.<sup>105</sup>

nonlinear least-squares method.<sup>105</sup> The mole fraction range used in the analysis is  $0 < x_A < 0.6$ , since solutions with higher CO<sub>2</sub> mole fractions (about  $> 0.7$ ) become immiscible liquids, as mentioned earlier. Trial-and-error analyses show that only one type of the complex (AB<sub>2</sub>) is dominating in the present liquid solution (CO<sub>2</sub> + [C<sub>2</sub>C<sub>2</sub>im][C<sub>1</sub>CO<sub>2</sub>]). This fact is consistent with the observation of the minimum  $G^E$  location of about  $x_A = 0.33$  shown in Figure 6 and consistent with the mechanism shown in Figure 5 that two moles of [C<sub>2</sub>C<sub>2</sub>im][C<sub>1</sub>CO<sub>2</sub>] are required per mole of CO<sub>2</sub> (2:1 [C<sub>2</sub>C<sub>2</sub>im][C<sub>1</sub>CO<sub>2</sub>]:CO<sub>2</sub>).<sup>105–108</sup> This highly asymmetric phase behavior with respect to concentration is extremely rare,<sup>115</sup> and one of the only other known examples is a binary system of HCl and water.<sup>115,116</sup> Similar behavior has been calculated for the CO<sub>2</sub> + [C<sub>2</sub>C<sub>1</sub>im][C<sub>1</sub>CO<sub>2</sub>] and CO<sub>2</sub> + [C<sub>4</sub>C<sub>1</sub>im][C<sub>1</sub>CO<sub>2</sub>] binary systems.<sup>103,104</sup> It is important to mention that in all three cases ([C<sub>2</sub>C<sub>1</sub>im][C<sub>1</sub>CO<sub>2</sub>], [C<sub>2</sub>C<sub>2</sub>im][C<sub>1</sub>CO<sub>2</sub>], [C<sub>4</sub>C<sub>1</sub>im][C<sub>1</sub>CO<sub>2</sub>]) the binary systems show the liquid–liquid separation (immiscibility) at high CO<sub>2</sub> concentrations (higher than about 0.7 mole fraction CO<sub>2</sub>).<sup>103–105</sup>

## Gas Separation

An EOS model for a ternary system has been developed to evaluate the effectiveness of ILs for gas separation.<sup>117–123</sup> Pure component and binary interaction parameters can be determined using the same procedures as discussed for the RK EOS model; however, the phase behavior prediction of the *ternary system* may not always be guaranteed based on the binary interaction parameters alone. In particular for systems containing supercritical fluids and/or nonvolatile compounds such as ILs, the validity of an EOS model for ternary mixtures must be checked experimentally. Ternary VLE experiments are not widely available in the literature and are a very sensitive check of the EOS model.

There have been an extremely large number of experimental and computational studies devoted to the solubility of CO<sub>2</sub> in ILs.<sup>124</sup> Much of this has been driven by the concept of using ILs for CO<sub>2</sub> capture. Most work in this area has focused on determining pure component isotherms for CO<sub>2</sub> and other gases such as N<sub>2</sub>, O<sub>2</sub>, and H<sub>2</sub>O. To understand the ability of an IL to separate CO<sub>2</sub> from other gases such as N<sub>2</sub>, however, one needs to perform mixed gas experiments or simulations. It is much more difficult to perform mixed gas experimental solubility measurements than pure component studies, and so most studies have focused on pure gas solubilities and assumed ideal mixing to estimate the separation capacity of an IL for a mixed-gas system.<sup>125,126</sup> Such an approximation is probably justified when gas solubility is low, such that the solution behaves ideally. As gas solubility increases, however, it is unlikely that pure gas solubilities can predict mixed gas solubilities with a high degree of accuracy. What is needed are more experimental and computational studies devoted to mixed gas solubilities in ILs.

One system where this has been done is gas mixtures of N<sub>2</sub>O and CO<sub>2</sub> in the IL (1-butyl-3-methylimidazolium acetate [C<sub>4</sub>C<sub>1</sub>im][C<sub>1</sub>CO<sub>2</sub>]), but there are other systems.<sup>117–123</sup> Ternary VLE measurements were performed using a GC method to analyze the vapor composition which confirmed the validity of the ternary EOS model.<sup>117–123</sup> Figure 7 is a  $PTx$  phase diagram for N<sub>2</sub>O + [C<sub>4</sub>C<sub>1</sub>im][C<sub>1</sub>CO<sub>2</sub>] which shows physical absorption

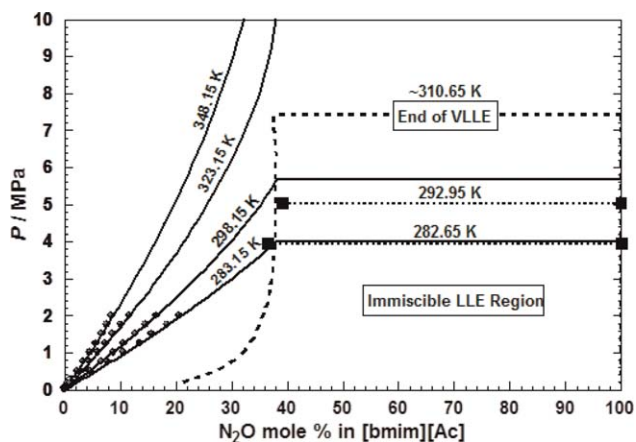


**Figure 7. Isothermal  $P_x$  phase diagram for N<sub>2</sub>O + [bmim][Ac] (i.e., [C<sub>4</sub>C<sub>1</sub>im][C<sub>1</sub>CO<sub>2</sub>]).**

Solid lines: calculated using the EOS model.<sup>123</sup> Symbols: ●, VLE data<sup>123</sup>; ■, VLE data<sup>123</sup>; figure was used with permission.<sup>123</sup>

with a large immiscibility (LLE) region that suggests this binary system likely exhibits Type III phase behavior. The CO<sub>2</sub> + [C<sub>4</sub>mim][C<sub>1</sub>CO<sub>2</sub>] system was previously measured<sup>103</sup> and the VLE data for N<sub>2</sub>O + CO<sub>2</sub> was obtained from the literature.<sup>127</sup>

Now that the present EOS model has been verified, the solubility behavior of the present ternary system can be predicted with confidence. To assess the feasibility of the gas separation by extractive distillation or selective absorption processes, the selectivity  $\alpha_{A/B}$  for gases A and B in the gas phase, or the absorption selectivity  $S_{B/A}$  for A and B in the liquid phase is commonly defined

$$\alpha_{A/B} = S_{B/A} = \left( \frac{y_A}{x_A} \right) / \left( \frac{y_B}{x_B} \right) \quad (14)$$

where  $x_A$  (or  $x_B$ ) and  $y_A$  (or  $y_B$ ) are the mole fractions of A (or B) in the liquid phase and vapor phase, respectively.<sup>128</sup> For this example, N<sub>2</sub>O is A and CO<sub>2</sub> is B. The N<sub>2</sub>O/CO<sub>2</sub> selectivity ( $\alpha_{A/B}$ ) in the gas phase has been examined using the present EOS model at various  $T$ ,  $P$ , and feed compositions.<sup>123</sup> In Figure 8a, the N<sub>2</sub>O/CO<sub>2</sub> selectivity ( $\alpha_{A/B}$ ) is plotted as a function of the IL [C<sub>4</sub>mim][C<sub>1</sub>CO<sub>2</sub>] concentration for ternary mixtures with three N<sub>2</sub>O/CO<sub>2</sub> mole ratios (3/1, 1/1, and 1/3) at  $T = 298.15$  K and  $P = 0.1$  MPa. The selectivity ( $\alpha_{A/B}$ ) increases dramatically with the addition of the IL [C<sub>4</sub>C<sub>1</sub>im][C<sub>1</sub>CO<sub>2</sub>] (greater than ca. 60 mole%).

To understand the change in selectivity due to the IL addition, Figure 8b provides clear insights, showing the selectivity *without* [C<sub>4</sub>C<sub>1</sub>im][C<sub>1</sub>CO<sub>2</sub>] at 298.15 K as a function of pressure for the same N<sub>2</sub>O/CO<sub>2</sub> feed ratios (3/1, 1/1, and 1/3). The selectivity enhancement due to the IL addition can be easily observed from the comparison between Figures 8a, b. The three feed ratios (3/1, 1/1, and 1/3) with the IL have a selectivity of about  $1 \times 10^3$  to  $1 \times 10^7$ , while the corresponding case *without* the IL shows a selectivity of about 0.96. Without the use of the IL the N<sub>2</sub>O/CO<sub>2</sub> separation is not practical.

Previous work using [C<sub>4</sub>C<sub>1</sub>im][BF<sub>4</sub>] as the entrainer achieved only a selectivity of 1.5.<sup>122</sup> The 3 to 7 orders of magnitude increase in selectivity using [C<sub>4</sub>C<sub>1</sub>im][C<sub>1</sub>CO<sub>2</sub>] shows

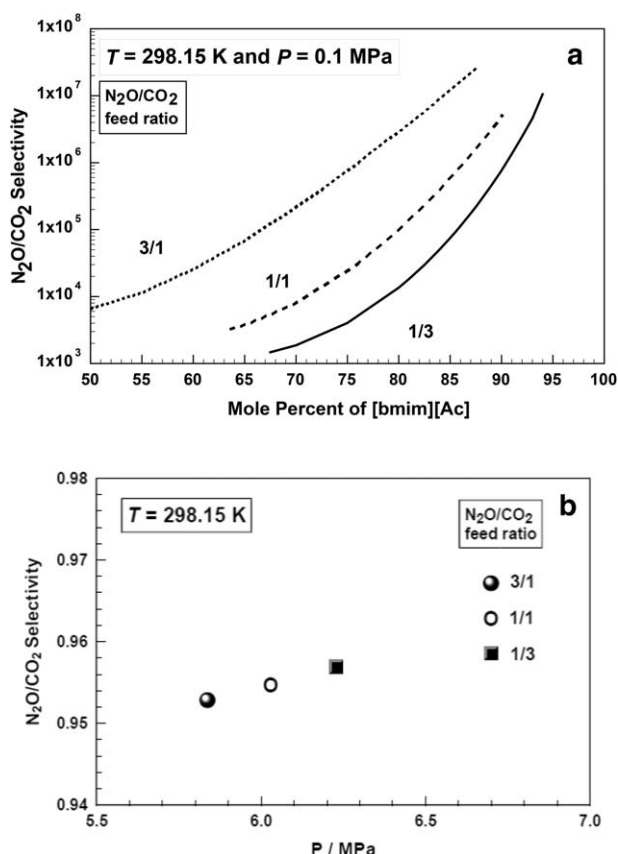


**Figure 8.** (a) Plots of calculated  $N_2O(A)/CO_2$ , (B) selectivity defined by Eq. (14) versus overall  $[bmim][Ac]$  (i.e.,  $[C_4C_1im][C_1CO_2]$ ), (C) mole fraction with three different  $N_2O/CO_2$  feed ratios at  $T = 298.15$  K and  $P = 0.1$  MPa.

(b) Selectivity plots without IL  $[bmim][Ac]$  (i.e.,  $[C_4C_1im][C_1CO_2]$ ) as a function of total pressure. Three cases with different  $N_2O/CO_2$  feed ratios are shown at  $T = 298.15$  K. Lines: dotted line, 3/1  $N_2O/CO_2$  feed mole ratio; broken line, 1/1  $N_2O/CO_2$  feed mole ratio; solid line, 1/3  $N_2O/CO_2$  feed mole ratio. Figures were used with permission.<sup>123</sup>

the significance that the choice of IL can make in this separation. As shown in Figures 4 and 5, the acetate containing ILs chemically interact with  $CO_2$ .<sup>103–106</sup> This strong chemical attraction significantly increases the selectivity over  $N_2O$  which demonstrates physical absorption behavior as shown in Figure 7. To our knowledge this is the *largest selectivity difference* ( $\alpha = 1 \times 10^3$  to  $1 \times 10^7$ ) ever demonstrated for a gas separation using an IL and clearly shows the utility of these novel materials as entrainers.

Although  $N_2O$  is not the major contributor to global warming (~6%), it is one of six greenhouse gases ( $CO_2$ ,  $CH_4$ ,  $N_2O$ , HFC, PFC, and  $SF_6$ ) identified for reduction by the United Nations Framework on Climate Change (UNFCCC).<sup>129</sup> As a result, a number of industries have voluntarily initiated efforts to reduce  $N_2O$  emissions, particularly from power plants and adipic acid production; therefore, ILs may play an important role in the separation of  $N_2O$  from  $CO_2$ .<sup>123</sup>

## Predictive Computational Modeling of Gas Solubility in ILs

Given the huge number of possible ILs and the time and expense associated with conducting detailed experimental solubility measurements, a great deal of effort has been directed at developing theoretical or computational methods that can predict phase equilibria for gas-IL systems. Almost all of these methods can be classified into one of three categories: (1) correlative methods that relate molecular-level descriptors to limited experimental data; (2) hybrid quantum chemical/statistical thermodynamics approaches; and (3) atomistic force field-based simulation methods. The latter two categories are the most “predictive” since, in principle, they do not require experimental data as input. They are also the most computationally intensive. The correlative methods are extremely fast, but do require significant amounts of experimental data and often do not extend well beyond the classes of systems for which the models were developed. A short review of each approach is provided next along with possible limitations and future developments of the methods.

### Correlative methods

Correlative methods seek to find statistical relationships between a property of interest (i.e., gas or vapor solubility) and a set of molecular descriptors that describe such things as the structural, topological, chemical and electronic characteristics of the molecules under consideration. The idea is to develop the correlations on a training set of experimental data and then apply it to make predictions for similar compounds outside the training set. These methods are generally referred to as quantitative structure property relationship (QSPR) models<sup>130</sup> and have been shown to do an excellent job correlating (and in some cases, predicting) gas solubility in ILs.

Eike et al.<sup>131</sup> were the first to use QSPR to estimate the solubility of organic solutes in ILs. They proposed a set of four-parameter QSPR models for the infinite-dilution activity coefficients  $\gamma^\infty$  of 38 organic solutes in three different ILs. These systems were chosen because high-quality experimental data were available from the Heintz group.<sup>74–76</sup>

Other researchers have carried out similar studies. Tämm and Burk<sup>132</sup> developed an improved QSPR model for the same system as that studied by Eike et al. using only three parameters. Katritzky et al. developed two- to four-parameter models for the partition coefficients of organic solutes in eight different ILs.<sup>133</sup> Recently, QSPR models have been used to examine  $CO_2$ <sup>134,135</sup> and  $H_2S$ <sup>136</sup> solubility in ILs.

In a related approach, QSPR correlations have been developed for gas-to-solvent and water-to-solvent partition coefficients for a range of solute-IL systems using the Abraham model,<sup>137</sup> in which the descriptors are the excess molar refraction and dipolarity/polarity of the solute, the solute hydrogen-bond acidity and hydrogen bond basicity, and the McGowan volume of the solute.<sup>138</sup> This approach correlates experimental data very well, but like other QSPR methods, it suffers from the fact that a separate QSPR expression is required for each IL. This prevents one from “designing” new ILs with a desired  $\gamma^\infty$  for a given solute. To overcome this, various group contribution methods have been proposed in which cation- and anion-specific coefficients are determined and used in a linear solvation model.<sup>139</sup> These methods all used relatively simple

multilinear models to perform the correlations, and accuracies within 20%–30% of experimental data were typically obtained.

Advanced neural networks and machine learning techniques have also been applied to develop more robust models for solubility in ILs.<sup>140–143</sup> Padaszyński has reviewed much of this and previous QSPR work and then used three different machine learning algorithms to develop new QSPR models for infinite dilution activity coefficients in ILs.<sup>144</sup> As neural network and machine learning techniques continue to advance, it is likely that they will play an increasingly important role in developing highly accurate solubility models. Crucial to this effort, however, is the availability of extensive, validated data. Up until now, only experimental solubility data have been used in developing these models; it will be interesting if some of the data generated by other methods is used to estimate solubilities (described below) in the future when developing these models.

### *Hybrid quantum/statistical thermodynamics methods*

Solvation is a collective phenomenon involving a complex interplay of interactions between the solute and the solvent molecules. Physics-based predictive models must account for these interactions. While quantum chemical methods can obtain very accurate energies of interaction between individual molecules, they are difficult to apply directly to compute solubilities for two reasons. First, solvation effects involve specific interactions between many molecules, making the use of highly accurate quantum methods expensive. Second, to properly consider entropic effects, a large number of configurations of the solute and solvent molecules should be sampled. Again, such calculations are prohibitively expensive with brute force quantum chemical methods. Researchers have attempted to use small cluster models to understand solvation trends<sup>145</sup> but the results are typically qualitative and do not provide macroscopic solubility predictions. As a result, approximate solvation models are often used in combination with quantum chemical methods to predict solvation. For example, Cramer, Truhlar, and coworkers<sup>146</sup> have extended their continuum SMD solvation model to ILs and used it to estimate solvation free energies for a number of solutes in twelve different ILs. The method requires as input several experimental properties of the IL, including dielectric constant, refractive index, surface tension, and acidity and basicity parameters. To our knowledge, this approach has only been applied to examine the solubility of organic species, but has not been applied to examine gas solubility in ILs.

Perhaps the most popular approach for modeling solubility that utilizes a quantum calculation in conjunction with a continuum treatment of the solvent is based on the CONductor-like Screening MOdel (COSMO). Klamt and coworkers<sup>147</sup> were the first to apply the COSMO-RS model in a “real solvent” manner (hence the “RS” suffix) to study the solubility of organic molecules in ILs. Briefly, the method involves carrying out quantum mechanical calculations on individual solutes in a conducting “continuum” which eliminates the need to explicitly model solvent molecules. The resulting geometries and surface charge densities are used to compute the interactions with the solvent (IL) via pairwise interacting surface segments. A statistical thermodynamic approach is then used to

estimate solute activity coefficients. Details of the procedure can be found in a review by Diedenhofen and Klamt.<sup>148</sup> The COSMO-RS method is attractive because it is relatively fast and so can be used to virtually screen solubility in ILs for different classes of solutes.

Klamt and coworkers<sup>147</sup> examined the same 38 organic compounds and 3 ILs for which experimental infinite dilution activity coefficient data were available.<sup>74–76</sup> They found that the method gave very good qualitative and, in many cases, quantitative agreement with experiment. Since then, there have been dozens of papers published in which COSMO-RS has been applied to examine solubilities in ILs. Applications involve screening studies to identify the best IL for the extraction of alkenes from alkanes<sup>149,150</sup> and alcohols from water,<sup>151</sup> among other applications. The predictive capability of the COSMO-RS model for 15 gases in 27 ILs was evaluated by Youngs and coworkers.<sup>152</sup> It was found that COSMO-RS can generally provide qualitative predictions of gas solubility, but quantitative results were sometimes lacking. For some systems, even qualitative trends were not captured. This points out the limitations of methods that fail to characterize the specific interactions that are important for solvation.

A variation of the basic COSMO approach (the so-called COSMO-SAC method,<sup>153</sup> where SAC stands for “segment activity coefficient”) has been used to screen ILs for possible use as CO<sub>2</sub> capture solvents.<sup>154</sup> A total of 65 cations and 32 anions were examined, forming a total of 2080 distinct ILs. Estimated Henry’s Law constants agreed reasonably well with available experimental data. Padaszyński has written an excellent comprehensive review on the use of COSMO-RS for predicting solvation, which we highly recommend.<sup>155</sup>

### *Atomistic force field methods*

Atomistic simulations have also been used extensively to model gas solubility in ILs. This approach treats all the molecular-level interactions explicitly, thereby overcoming some of the limitations of implicit or continuum solvation models. To treat such systems in a computationally efficient manner, an approximate classical representation of the energetics (a “force field”) is used. Molecular dynamics or Monte Carlo methods are used to provide statistical sampling of conformations.

The very first attempt at modeling solubility in ILs was carried out using an atomistic force field-based simulation. Lynden-Bell and coworkers<sup>156,157</sup> used molecular dynamics to calculate the interactions and excess chemical potential of water, methanol, dimethyl ether and propane in 1,3-dimethylimidazolium chloride. Because their calculations treated the interactions between the solute and solvent explicitly, they were able to provide molecular-level explanations for some of the solvation trends they observed. For example, they found that the solute hydroxyl groups associated mainly with the chloride anion, and that each water molecule associated with two chloride ions via hydrogen bonding interactions. The ether and alkane did not associate strongly with the anion, and cation arrangement about the solutes was diffuse. This work confirmed the importance of electrostatic interactions and hydrogen bonding on solvation. The detailed information on specific interactions responsible for solvation trends obtained from this method suggested that such techniques could not

only make solvation predictions, but could also provide guidance as to the physical interactions that were most important in determining solubility. Many subsequent atomistic calculations of infinite dilution solubility were carried out using a variety of approaches; in general, these methods agree reasonably well with experimental data.<sup>158–160</sup>

Atomistic simulations enable one to compute not just infinite dilution properties but also full isotherms, which as noted earlier is crucial. Maurer and coworkers were the first to compute an isotherm for a gas in an IL.<sup>161,162</sup> They used isobaric Gibbs ensemble Monte Carlo to estimate the solubility of O<sub>2</sub>, CO<sub>2</sub>, CO, and H<sub>2</sub> in the IL [C<sub>4</sub>C<sub>1</sub>im][PF<sub>6</sub>]. Subsequent work has shown that quantitative results can be obtained for CO<sub>2</sub>,<sup>163–165</sup> NH<sub>3</sub>,<sup>166</sup> sulfur compounds,<sup>167</sup> and light hydrocarbons.<sup>168</sup> Water poses a particular problem for atomistic simulations; commonly used fixed charge force fields fail to capture experimental absorption isotherms. It is likely that more advanced force fields that treat solute and solvent polarizability are needed.<sup>169</sup> The absorption of gas mixtures can also be readily simulated with these methods<sup>170</sup>; this is a major advantage because mixed gas experiments are significantly more difficult to conduct than pure gas experiments as discussed previously.

These and other studies have demonstrated that the physical solubility of gases in ILs can be modeled accurately using atomistic-level simulations. Force fields for solutes and many ILs are readily available,<sup>171,172</sup> and the steady increase in computing power has meant that the time and expense for performing these calculations continues to decrease. Classical atomistic force field-based methods are the most predictive and accurate approaches for determining macroscopic solubility of gases in ILs, but they are also the most computationally intensive. They enable the estimation of infinite dilution solvation behavior as well as full isotherms. Quantum methods that approximate the solvent as a continuum enable qualitative and in some cases quantitative estimates of solvation free energies and infinite dilution behavior. They are particularly well suited for screening studies where relative solubilities are most important. QSPR methods are fast and effective when a significant amount of experimental data are available. They enable data correlation in terms of a small number of easily determined descriptors.

Advances in predictive methods for gas solubility in ILs will likely not rely on any one method, but will instead leverage computing power advances to develop improved machine learning algorithms, better force fields, and improved simulation algorithms. Computational methods of the kind described here are an important complement to experimental measurements for determining physical solubility of gases in ILs. Treating reactive systems such as the CO<sub>2</sub>/acetate anion described earlier or task-specific ILs<sup>173</sup> remains a major challenge for the modeling community and advanced methods are required to model such systems.

## Concluding Remarks

A deeper understanding of molecular interactions between gases and ILs is still required. The focus on the solubility of important industrial gases in ILs must now include transport and calorimetric measurements. Only a few articles have been published on diffusion measurements<sup>50,92–94,174–176</sup> and enthalpies

of dissolution<sup>105,177</sup> in ILs. Typical diffusion coefficients for CO<sub>2</sub> in imidazolium-based ILs range from  $1 \times 10^{-5}$  to  $1 \times 10^{-6}$  cm<sup>2</sup> s<sup>-1</sup> and heats of mixing from a few kJ mol<sup>-1</sup> (physical sorption) to 30–40 kJ mol<sup>-1</sup> (chemical sorption).<sup>105</sup> Gas–liquid interfaces are also being studied and experiments have shown interfacial water uptake is much more rapid at the surface than in the bulk.<sup>178</sup> Heat of mixing calculations using EOS models are only semiquantitative; therefore, experimental measurements are needed to develop process simulations and accurate economic models.

Theoretical methods such as QSPR and COSMO-RS have been used to perform screening studies to search for new ILs with certain solvation characteristics, while atomistic simulations and quantum chemical calculations have provided molecular-level details that have greatly enhanced our understanding of solvation in ILs. The reliability and accuracy of these methods is generally good, but the range of systems investigated is still very small. More benchmark studies are needed where experimental measurements and modeling studies are carried out on a range of well-characterized systems. In general, these methods are not able to handle reactive systems (i.e., chemical absorption)<sup>173</sup> in a direct manner, although a number of advances have been made.<sup>179–181</sup>

New materials are also being developed for gas sensors,<sup>182,183</sup> supported IL membranes (SILMs) and poly(IL) membranes,<sup>184–187</sup> carbon capture<sup>188–190</sup> and chemical reaction using supported IL phases (SILPs), where the IL is confined on the surface or in the pores of the material.<sup>191–194</sup> Professor Daniel Armstrong at the University of Texas in Arlington has developed a new class of capillary GC columns with stationary phases based on ILs. His group has synthesized dicationic and polycationic ILs which are stable to water and oxygen even at high temperatures.<sup>195</sup> A variety of capillary GC columns are now available based on IL technology.<sup>196</sup>

In the past couple of years (2015–2016), we have also seen some of the largest scale IL processes announced which require knowledge of gas solubility. First, Queens University Ionic Liquids Laboratory in collaboration with the Malaysian oil and gas company, Petronas, has developed an IL process for the efficient scrubbing of mercury vapor from natural gas.<sup>197,198</sup> The process is now operating on an industrial scale using chlorocuprate (II) ILs impregnated on high surface area porous solid supports. The SILP approach to heterogenize the IL allowed the material to be used in standard industrial-scale mercury removal equipment and the rapid commercialization of the process. The SILP containing IL outperformed the incumbent activated carbon and better manages process upsets such as spikes in mercury concentration.

Chevron announced in October, 2016, the development of a new chloroaluminate IL alkylation process.<sup>199–201</sup> The chloroaluminate ILs provide high activity, selectivity and catalyst stability for C<sub>4</sub> alkylation and provide Chevron with an alternative to using corrosive and toxic hydrofluoric acid as a catalyst.

Molecular-level understanding of the gas-IL interactions is still in progress and should provide future insight into the detailed liquid structure that can guide new experiments. Once an application and IL are identified, several other properties must still be evaluated.<sup>28</sup> First, the cost of the IL and financial benefit must be calculated and clearly provide a value

proposition compared with the incumbent technology. The chemical stability of the IL must be demonstrated in the presence of the gases (and impurities) at operating conditions and required time scales. Materials of construction, corrosion, transport limitations, foaming, toxicity, waste handling, to name a few, are additional details that must also be considered.<sup>28</sup> Traditional unit operations (i.e., columns and tanks) may be employed, but new materials such as SILMs should also be considered. Although IL-based processes share the same hurdles to development and commercialization as any new chemical process, it is our belief that ILs still hold the possibility for future gas separation, chemical reaction, and many other new applications.<sup>202</sup>

## Acknowledgments

Mark Shiflett would like to dedicate this article to his colleague and friend, Dr. Akimichi Yokozeki, who developed the EOS method and association model described herein. Mark Shiflett was extremely thankful and blessed to have known and worked with Michi for 25 years. A verse from the Bible, Psalms 32:8, best summarizes his relationship to Mark Shiflett. "I will instruct you and guide you along the best pathways for your life; I will advise you and watch your progress." (In Loving Memory of Akimichi "Michi" Yokozeki, December 25, 1942 to April 9, 2014). Mark Shiflett acknowledges support from the DuPont Company, and Edward Maginn acknowledges support from the Air Force Office of Scientific Research under AFOSR Award No. FA9550-14-1-0306.

## Literature Cited

1. Freemantle M. *An Introduction to Ionic Liquids*. Royal Society of Chemistry, 2010.
2. Friedel C, Crafts JM. Sur une nouvelle méthode générale de synthèse d'hydrocarbures, d'acétones, etc. *Compt Rend*. 1877;84:1392–1450.
3. Nambu N, Hiraoka N, Shigemura K, Hamanaka S, Ogawa M. A Study of the 1,3,5-Trialkylbenzenes with Aluminum Chloride-Hydrogen Chloride Systems. *Bull Chem Soc Jpn*. 1976;49:3637–3640.
4. Walden P. Molecular weights and electrical conductivity of several fused salts. *Izv Imp Akad Nauk (Bull. Acad. Imp. Sci. St. Petersburg)*. 1914;8:405–422.
5. Wilkes JS, Zaworotko MJ. Air and water stable 1-ethyl-3-methylimidazolium based ionic liquids. *Chem Soc Chem Commun*. 1992;13:965–967.
6. Wilkes JS. A short history of ionic liquids—from molten salts to neoteric solvents. *Green Chem*. 2002;4:73–80.
7. Rogers RD, Seddon KR. *Ionic Liquids: Industrial Applications to Green Chemistry*. ACS Publications, 2003.
8. Wasserscheid P, Welton T. *Ionic Liquids in Synthesis*. Wiley-Vch, 2003.
9. Rogers RD, Seddon KR. *Ionic Liquids as Green Solvents. Progress and Prospects*. ACS Publications, 2003: 856.
10. Brazel CS, Rogers RD. *Ionic Liquids in Polymer Systems: Solvents, Additives, and Novel Applications*. ACS Publications, 2005.
11. Rogers RD, Seddon KR. *Ionic Liquids IIIA: Fundamentals, Progress, Challenges, and Opportunities*. ACS Publications, 2005:901.
12. Rogers RD, Seddon KR. *Ionic Liquids IIIB: Transformations and Processes*. OUP, 2005.
13. Ohno H. *Electrochemical Aspects of Ionic Liquids*. John Wiley & Sons, 2005.
14. Letcher TM. *Development and Applications in Solubility*. Royal Society of Chemistry, 2007.
15. Wasserscheid P, Welton T. *Ionic Liquids in Synthesis, vol. 1*. John Wiley & Sons, 2008.
16. Wasserscheid P, Welton T. *Ionic Liquids in Synthesis, vol. 2*. John Wiley & Sons, 2008.
17. Koel M. *Ionic Liquids in Chemical Analysis*. CRC Press, 2008.
18. Endres F, MacFarlane D, Abbott A. *Electrodeposition from Ionic Liquids*. John Wiley & Sons, 2008.
19. Plechkova NV, Rogers RD, Seddon KR. *Ionic Liquids: from Knowledge to Application*. ACS Publications, 2009: 1030.
20. Kirchner B. *Ionic Liquids*. Springer, 2009:290.
21. Gaune-Escard M, Seddon KR, editors. *Molten Salts and Ionic Liquids: Never the Twain?* John Wiley & Sons, 2010.
22. Malhotra SV, editor. *Ionic Liquid Applications: Pharmaceuticals, Therapeutics, and Biotechnology*. ACS Publications, 2010.
23. Trulove P, Mantz R, De Long HC, editors. *Physical and Analytical Electrochemistry in Ionic Liquids*. Electrochemical Society, 2010.
24. Ohno H. *Electrochemical Aspects of Ionic Liquids*. John Wiley & Sons, 2011.
25. Kokorin A, editor. *Ionic Liquids: Applications and Perspectives*. InTech, 2011.
26. Rogers RD, Seddon KR, Volkov S. *Green Industrial Applications of Ionic Liquids*. Springer Science & Business Media, 2012:92.
27. Dominguez de Maria P, editor. *Ionic Liquids in Biotransformations and Organocatalysis: Solvents and Beyond*. John Wiley & Sons, 2012.
28. Plechkova NV, Seddon KR. *Ionic Liquids Uncoiled: Critical Expert Overviews*. John Wiley & Sons, 2013.
29. Fehrmann R, Riisager A, Haumann M. *Supported Ionic Liquids: Fundamentals and Applications*. John Wiley & Sons, 2013.
30. Fang Z, Smith RL Jr, Qi X. *Production of Biofuels and Chemicals with Ionic Liquids, vol. 1*. Springer Science & Business Media, 2013.
31. Kadokawa J, editor. *Ionic Liquids-New Aspects for the Future*. InTech, 2013.
32. Plechkova NV, Seddon KR. *Ionic Liquids further UnCOILED: Critical Expert Overviews*. John Wiley & Sons, 2014.
33. De Los Rios AP, Fernandez FJH. *Ionic Liquids in Separation Technology*. Elsevier, 2014.
34. Plechkova NV, Seddon KR. *Ionic Liquids Completely Uncoiled: Critical Expert Overviews*. John Wiley & Sons, 2015.
35. Dupont J, Itoh T, Lozano P, Malhotra SV, editors. *Environmentally Friendly Syntheses Using Ionic Liquids*. CRC Press, 2015.
36. Bogel-Lukasik R, editor. *Ionic Liquids in the Biorefinery Concept: Challenges and Perspectives*. Royal Chemical Society, 2016:36.
37. Kazakov A, Magee JW, Chirico RD, Paulechka E, Diky V, Muzny CD, Kroenlein K, Frenkel M. *NIST Standard*

Reference Database 147: NIST Ionic Liquids Database (ILThermo), Version 2.0. 2017, Gaithersburg, MD: National Institute of Standards and Technology. Available from <http://ilthermo.boulder.nist.gov>.

38. Dong Q, Muzny CD, Kazakov A, Diky V, Magee JW, Widegren JA, Chirico RD, Marsh KN, Frenkel M. ILThermo: a free-access web database for thermodynamic properties of ionic liquids. *J Chem Eng Data*. 2007; 52(4):1151–1159.
39. Lei Z, Dai C, Chen B. Gas solubility in ionic liquids. *Chem Rev*. 2014;114:1289–1326.
40. Shiflett MB, Yokozeki A. Solubility of fluorocarbons in room temperature ionic liquids. In: Plechkova NV, Rogers RD, Seddon KR, editors. *Ionic Liquids: From Knowledge to Application*, ACS Symposium Series No. 1030. Washington, D.C.: American Chemical Society, 2009:21–42.
41. Shiflett MB, Yokozeki A. Solubility of gases in ionic liquids. In: Seddon KR, editor. *Ionic Liquids: UnCOILed*, ACS Symposium Series. Plechkova, NV: John Wiley & Sons, 2013:349–386.
42. Scott RL, van Konynenburg PH. Static problems of solutions. Van der Waals and related models for hydrocarbon mixtures. *Discuss Faraday Soc*. 1970;49:87–97.
43. van Konynenburg PH, Scott RL. Critical lines and phase equilibria in binary van der Waals mixtures. *Philos. Trans*. 1980;A298:495–540.
44. Battino R, Clever HL. The solubility of gases in water and seawater. In: Letcher TM, editor. *Developments and Applications in Solubility*. Cambridge, UK: Royal Society of Chemistry Publishing, 2007:66–78.
45. Marsh KN, Brennecke JF, Chirico RD, Frenkel M, Heintz A, Magee JW, Peters CJ, Rebelo LPN, Seddon KR. Thermodynamic and thermophysical properties of the reference ionic liquid: 1-hexyl-3-methylimidazolium bis[(trifluoromethyl)sulfonyl]amide (including mixtures). Part 1. Experimental methods and results. *Pure Appl Chem*. 2009;81:781–790.
46. Chirico RD, Diky V, Magee JW, Frenkel M, Marsh KN. Thermodynamic and thermophysical properties of the reference ionic liquid: 1-hexyl-3-methylimidazolium bis[(trifluoromethyl)sulfonyl]amide (including mixtures). Part 2. Critical evaluation and recommended property values. *Pure Appl Chem*. 2009;81:791–828.
47. Anthony JL, Maginn EJ, Brennecke JF. Solution thermodynamics of imidazolium-based ionic liquids and water. *J Phys Chem B*. 2001;105:10942–10949.
48. Anthony JL, Maginn EJ, Brennecke JF. Solubilities and thermodynamic properties of gases in the ionic liquid 1-n-butyl-3-methylimidazolium hexafluorophosphate. *J Phys Chem B*. 2002;106:7315–7320.
49. Cadena C, Anthony JL, Shah JK, Morrow TI, Brennecke JF, Maginn EJ. Why is CO<sub>2</sub> so soluble in imidazolium-based ionic liquids? *J Am Chem Soc*. 2004;126:5300–5308.
50. Shiflett MB, Yokozeki A. Solubilities and diffusivities of carbon dioxide in ionic liquids: [bmim][PF<sub>6</sub>] and [bmim][BF<sub>4</sub>]. *Ind Eng Chem Res*. 2005;44:4453–4464.
51. Hiden Isochema Ltd. Warrington, United Kingdom. Available from [www.hiddenisochema.com](http://www.hiddenisochema.com).
52. Carvalho PJ, Alvarez VH, Schröder B, Gil AM, Marrucho IM, Aznar M, Santos LMNBF, Coutinho JAP. Specific solvation interactions of CO<sub>2</sub> on acetate and trifluoroacetate imidazolium based ionic liquids at high pressures. *J Phys Chem B*. 2009;113:6803–6812.
53. Carvalho PJ, Álvarez VH, Machado JJB, Pauly J, Daridon J, Marrucho IM, Aznar M, Coutinho JAP. High pressure phase behavior of carbon dioxide in 1-alkyl-3-methylimidazolium bis(trifluoromethylsulfonyl)imide ionic liquids. *J Supercrit Fluids*. 2009;48:99–107.
54. Carvalho PJ, Alvarez VH, Marrucho IM, Aznar M, Coutinho JAP. High pressure phase behavior of carbon dioxide in 1-butyl-3-methylimidazolium bis(trifluoromethylsulfonyl)imide and 1-butyl-3-methylimidazolium dicyanamide ionic liquids. *J Supercrit Fluids*. 2009;50: 105–111.
55. Carvalho PJ, Alvarez VH, Marrucho IM, Aznar M, Coutinho JAP. High carbon dioxide solubilities in trihexyltetradecylphosphonium-based ionic liquids. *J Supercrit Fluids*. 2010;52:258–265.
56. Shariati A, Peters CJ. High-pressure phase behavior of systems with ionic liquids: measurements and modeling of the binary system fluoroform + 1-ethyl-3-methylimidazolium hexafluorophosphate. *J Supercrit Fluids*. 2003;25:109–117.
57. Shariati A, Peters CJ. High-pressure phase behavior of systems with ionic liquids. Part II. The binary system carbon dioxide + 1-ethyl-3-methylimidazolium hexafluorophosphate. *J Supercrit Fluids*. 2004;29:43–48.
58. Shariati A, Peters CJ. High-pressure phase behavior of systems with ionic liquids. Part III. The binary system carbon dioxide + 1-hexyl-3-methylimidazolium hexafluorophosphate. *J Supercrit Fluids*. 2004;30:139–144.
59. Costantini M, Toussaint VA, Shariati A, Peters CJ, Kikic I. High-pressure phase behavior of systems with ionic liquids. Part IV. The binary system carbon dioxide + 1-hexyl-3-methylimidazolium tetrafluoroborate. *J Chem Eng Data*. 2005;50:52–55.
60. Kroon MC, Shariati A, Costantini M, Van Spronsen J, Witkamp G-J, Sheldon RA, Peters CJ. High-pressure phase behavior of systems with ionic liquids. Part V. The binary system carbon dioxide + 1-butyl-3-methylimidazolium tetrafluoroborate. *J Chem Eng Data*. 2005;50:173–176.
61. Song HN, Byung-Chul L, Lim JS. Measurement of CO<sub>2</sub> solubility in ionic liquids: [BMP][TfO] and [P14.6.6.6][Tf<sub>2</sub>N] by measuring bubble-point pressure. *J Chem Eng Data*. 2010; 55:891–896.
62. Maurer G, Pérez-Salado Kamps Á. Solubility of gases in ionic liquids, aqueous solutions, and mixed solvents. In: Letcher TM, editor. *Developments and Applications in Solubility*. Cambridge, UK: Royal Society of Chemistry, 2007:41–58.
63. Kumelan J, Tuma D, Pérez-Salado Kamps Á, Maurer G. Solubility of the single gases carbon dioxide and hydrogen in the ionic liquid [bmpy][Tf<sub>2</sub>N]. *J Chem Eng Data*. 2010;55:165–172.
64. Kumelan J, Tuma D, Pérez-Salado Kamps Á, Maurer G. Solubility of the single gases carbon monoxide and oxygen in the ionic liquid [hmim][Tf<sub>2</sub>N]. *J Chem Eng Data*. 2009;54:966–971.
65. Kumelan J, Pérez-Salado Kamps Á, Tuma D, Maurer G. Solubility of CO<sub>2</sub> in the ionic liquid [hmim][Tf<sub>2</sub>N]. *J Chem Thermodyn*. 2006;38:1396–1401.

66. Ren W, Scurto AM. High-pressure phase equilibria with compressed gases. *Rev Sci Instrum.* 2007;78:125104–125107.
67. Ren W, Scurto AM. Phase equilibria of imidazolium ionic liquids and the refrigerant gas 1,1,1,2-tetrafluoroethane (R-134a). *Fluid Phase Equilib.* 2009;286:1–7.
68. Ren W, Sensenich B, Scurto AM. High-pressure phase equilibria of {carbon dioxide (CO<sub>2</sub>) + n-alkyl-imidazolium bis(trifluoromethylsulfonyl)amide} ionic liquids. *J Chem Thermodyn.* 2010;42:305–311.
69. Husson-Borg P, Majer V, Costa Gomes MF. Solubilities of oxygen and carbon dioxide in butyl methyl imidazolium tetrafluoroborate as a function of temperature at pressures close to atmospheric pressure. *J Chem Eng Data.* 2003;48:480–485.
70. Jacquemin J, Costa Gomes MF, Husson P, Majer V. Solubility of carbon dioxide, ethane, methane, oxygen, nitrogen, hydrogen, argon, and carbon monoxide in 1-butyl-3-methylimidazolium tetrafluoroborate between temperatures 283 K and 343 K and at pressures close to atmospheric. *J Chem Thermodyn.* 2006;38:490–502.
71. Jacquemin J, Husson P, Majer V, Costa Gomes MF. Low-pressure solubilities and thermodynamics of solvation of eight gases in 1-butyl-3-methylimidazolium hexafluorophosphate. *Fluid Phase Equilib.* 2006;240:87–95.
72. Costa Gomes MF. Low-pressure solubility and thermodynamic of solvation of carbon dioxide, ethane, and hydrogen in 1-hexyl-3-methylimidazolium bis(trifluoromethylsulfonyl)amide between temperatures of 283 K and 343 K. *J Chem Eng Data.* 2007;52:472–475.
73. Pison L, Canongia Lopes JN, Rebelo LPN, Padua AAH, Costa Gomes MF. Interactions of fluorinated gases with ionic liquids: solubility of CF<sub>4</sub>, C<sub>2</sub>F<sub>6</sub>, and C<sub>3</sub>F<sub>8</sub> in trihexyltetradecylphosphonium bis(trifluoromethylsulfonyl)amide. *J Phys Chem B.* 2008;112:12394–12400.
74. Heintz A, Kulikov DV, Verevkin SP. Thermodynamic properties of mixtures containing ionic liquids. 1. Activity coefficients at infinite dilution of alkanes, alkenes, and alkylbenzenes in 4-methyl-*n*-butylpyridinium tetrafluoroborate using gas-liquid chromatography. *J Chem Eng Data.* 2001;46:1526–1529.
75. Heintz A, Kulikov DV, Verevkin SP. Thermodynamic properties of mixtures containing ionic liquids. Activity coefficients at infinite dilution of polar solutes in 4-methyl-*n*-butylpyridinium tetrafluoroborate using gas-liquid chromatography. *J Chem Thermodyn.* 2002;34:1341–1347.
76. Heintz A, Kulikov DV, Verevkin SP. Thermodynamic properties of mixtures containing ionic liquids. 2. Activity coefficients at infinite dilution of hydrocarbons and polar solutes in 1-methyl-3-ethyl-imidazolium bis(trifluoromethylsulfonyl) amide and in 1,2-dimethyl-3-ethyl-imidazolium bis(trifluoromethylsulfonyl) amide using gas-liquid chromatography. *J Chem Eng Data.* 2002;47:894–899.
77. Kazarian SG, Briscoe BJ, Welton T. Combining ionic liquids and supercritical fluids: in situ ATR-IR study of CO<sub>2</sub> dissolved in two ionic liquids at high pressures. *Chem Commun.* 2000;20:2047–2048.
78. Huang J, Riisager A, Berg RW, Fehrmann R. Tuning ionic liquids for high gas solubility and reversible gas sorption. *J Mol Catal A Chem.* 2008;279:170–176.
79. Shiflett MB, Yokozeki A. Vapor-liquid-liquid equilibria of pentafluoroethane and ionic liquid [bmim][PF<sub>6</sub>] mixtures studied with the volumetric method. *J Phys Chem B.* 2006;110:14436–14443.
80. Shiflett MB, Yokozeki A. Vapor-liquid-liquid equilibria of hydrofluorocarbons and 1-butyl-3-methylimidazolium hexafluorophosphate. *J Chem Eng Data.* 2006;51:1931–1939.
81. Wu C-T, Marsh KN, Deev AV, Boxall JA. Liquid-liquid equilibria of room-temperature ionic liquids and butan-1-ol. *J Chem Eng Data.* 2003;48:486–491.
82. Heintz A, Lehmann JK, Wertz C. Thermodynamic properties of mixtures containing ionic liquids. 3. Liquid-liquid equilibria of binary mixtures of 1-ethyl-3-methylimidazolium bis(trifluoromethylsulfonyl)imide with propan-1-ol, butan-1-ol, and pentan-1-ol. *J Chem Eng Data.* 2003;48:472–474.
83. Crosthwaite JM, Aki SNVK, Maginn EJ, Brennecke JF. Liquid-phase behavior of imidazolium-based ionic liquids with alcohols: effect of hydrogen bonding and non-polar interactions. *Fluid Phase Equilib.* 2005;228–229:303–309.
84. Crosthwaite JM, Aki SNVK, Maginn EJ, Brennecke JF. Liquid-phase behavior of imidazolium-based ionic liquids with alcohols. *J Phys Chem B.* 2004;108:5113–5119.
85. Wagner M, Stanga O, Schröder W. The liquid-liquid coexistence of binary mixtures of the room-temperature ionic liquid 1-methyl-3-hexylimidazolium tetrafluoroborate with alcohols. *Phys Chem Chem Phys.* 2004;6:4421–4431.
86. Wagner M, Stanga O, Schröder W. Corresponding states analysis of the critical points in binary solutions of room-temperature ionic liquids. *Phys Chem Chem Phys.* 2003;5:3943–3950.
87. Shiflett MB, Yokozeki A. Solubility of CO<sub>2</sub> in room-temperature ionic liquid [hmim][Tf<sub>2</sub>N]. *J Phys Chem B.* 2007;111:2070–2074.
88. Yokozeki A, Shiflett MB. Global phase behaviors of trifluoromethane in room-temperature ionic liquid [bmim][PF<sub>6</sub>]. *AIChE J.* 2006;52:3952–3957.
89. Van Ness CH, Abbott MM. *Classical Thermodynamics of Nonelectrolyte Solutions.* New York: McGraw-Hill, 1982.
90. Walas SM. *Phase Equilibria in Chemical Engineering.* Boston, MA: Butterworth, 1985:178–183.
91. Reid RC, Prausnitz JM, Poling RE. *The Properties of Gases and Liquids*, 4th ed. New York: McGraw-Hill, 1987.
92. Shiflett MB, Junk CP, Harmer MA, Yokozeki A. Solubility and diffusivity of difluoromethane in room-temperature ionic liquids. *J Chem Eng Data.* 2006;51:483–495.
93. Shiflett MB, Junk CP, Harmer MA, Yokozeki A. Solubility and diffusivity of 1,1,1,2-tetrafluoroethane in room-temperature ionic liquids. *Fluid Phase Equilib.* 2006;242:220–232.
94. Shiflett MB, Yokozeki A. Solubility and diffusivity of hydrofluorocarbons in room-temperature ionic liquids. *AIChE J.* 2006;52:1205–1219.
95. Yokozeki A. Solubility of refrigerants in various lubricants. *Int J Thermophys.* 2001;22:1057–1071.
96. Yokozeki A. Solubility correlation and phase behaviors of carbon dioxide + lubricant oil mixtures. *Appl Energy.* 2007;84:159–175.

97. Valderrama JO, Robles PA. Critical properties, normal boiling temperatures, and acentric factors of fifty ionic liquids. *Ind Eng Chem Res.* 2007;46:1338–1344.
98. Valderrama JO, Sanga WW, Lazzs JA. Critical properties, normal boiling temperatures, and acentric factors of another 200 ionic liquids. *Ind Eng Chem Res.* 2008;47:1318–1330.
99. Valderrama JO, Rojas RE. Critical properties of ionic liquids. *Revisited Ind Eng Chem Res.* 2009;48:6890–6900.
100. Rai N, Maginn EJ. Vapor-liquid coexistence and critical behavior of ionic liquids via molecular simulations. *J Phys Chem Lett.* 2011;2:1439–1443.
101. Rai N, Maginn EJ. Critical behavior and vapour-liquid coexistence of 1-alkyl-3-methylimidazolium bis(trifluoromethylsulfonyl)amide ionic liquids via Monte Carlo simulations. *Faraday Discuss.* 2011;154:1–18.
102. Rane KS, Errington JR. Using Monte Carlo simulation to compute liquid-vapor saturation properties of ionic liquids. *J Phys Chem B.* 2013;117:8018–8030.
103. Shiflett MB, Kasprzak DJ, Junk CP, Yokozeki A. Phase behavior of {carbon dioxide + [bmim][Ac]} mixtures. *J Chem Thermodyn.* 2008;40:25–31.
104. Yokozeki A, Shiflett MB, Junk CP, Grieco LM, Foo T. Physical and chemical absorptions of carbon dioxide in room-temperature ionic liquids. *J Phys Chem B.* 2008;112:16654–16663.
105. Shiflett MB, Elliott BA, Lustig SR, Subramaniam S, Kelkar MS, Yokozeki A. Phase behavior of CO<sub>2</sub> in room-temperature ionic liquid 1-ethyl-2-ethylimidazolium acetate. *ChemPhysChem.* 2012;13:1806–1817.
106. Maginn EJ. Design and evaluation of ionic liquids as novel CO<sub>2</sub> absorbents. *Quarterly Technical Report to DOE.* National Energy Technology Laboratory, report NT42122, Pittsburgh, PA.
107. Besnard M, Cabaco MI, Chávez FV, Pinaud N, Sebastião PJ, Coutinho JAP, Danten Y. On the spontaneous carboxylation of 1-butyl-3-methylimidazolium acetate by carbon dioxide. *Chem Commun.* 2012;9:1245–1247.
108. Gurau G, Rodríguez H, Kelley SP, Janiczek P, Kalb RS, Rogers RD. Demonstration of chemisorption of carbon dioxide in 1,3-dialkylimidazolium acetate ionic liquids. *Angew Chem Int Ed.* 2011;50:12024–12026.
109. Acree WE, Jr. *Thermodynamic Properties of Nonelectrolyte Solutions.* New York: Academic Press, 1984.
110. McGlashan ML, Rastogi RP. The thermodynamics of associated mixtures. Part 1.-Dioxan + chloroform. *Trans Faraday Soc.* 1958;54:496–501.
111. Ohta T, Asano H, Nagata I. Thermodynamic study of complex formation in four binary liquid mixtures containing chloroform. *Fluid Phase Equilib.* 1980;4:105–114.
112. Matusi T, Hepler LG, Fenby DV. Thermodynamic investigation of complex formation by hydrogen bonding in binary liquid systems. Chloroform with triethylamine, dimethyl sulfoxide, and acetone. *J Phys Chem.* 1973;77:2397–2400.
113. Handa YP, Fenby DV, Jones DE. Vapour pressures of triethylamine + chloroform and of triethylamine + dichloromethane. *J Chem Thermodyn.* 1975;7:337–343.
114. Hepler LG, Fenby DV. Thermodynamic study of complex formation between triethylamine and chloroform. *J Chem Thermodyn.* 1973;5:471–475.
115. Rowlinson JS, Swinton FL. *Liquids and Liquid Mixtures.* London: Butterworth, 1982.
116. Kao JTF. Vapor-liquid equilibrium of water-hydrogen chloride system. *J Chem Eng Data.* 1970;15:362–367.
117. Yokozeki A, Shiflett MB. Hydrogen purification using room-temperature ionic liquids. *Appl Energy.* 2007;84:351–361.
118. Yokozeki A, Shiflett MB. Separation of carbon dioxide and sulfur dioxide gases using room-temperature ionic liquid [hmim][Tf<sub>2</sub>N]. *Energy Fuels.* 2009;23:4701–4708.
119. Shiflett MB, Yokozeki A. Separation of carbon dioxide and sulfur dioxide using room-temperature ionic liquid [bmim][MeSO<sub>4</sub>]. *Energy Fuels.* 2010;24:1001–1008.
120. Shiflett MB, Yokozeki A. Separation of CO<sub>2</sub> and H<sub>2</sub>S using room-temperature ionic liquid [bmim][PF<sub>6</sub>]. *Fluid Phase Equilib.* 2010;294:105–113.
121. Shiflett MB, Niehaus AMS, Yokozeki A. Separation of CO<sub>2</sub> and H<sub>2</sub>S using room-temperature ionic liquid [bmim][MeSO<sub>4</sub>]. *J Chem Eng Data.* 2010;55:4785–4793.
122. Shiflett MB, Niehaus AMS, Yokozeki A. Separation of N<sub>2</sub>O and CO<sub>2</sub> using room-temperature ionic liquid [bmim][BF<sub>4</sub>]. *J Phys Chem B.* 2011;115:3478–3487.
123. Shiflett MB, Niehaus AMS, Yokozeki A. Separation of N<sub>2</sub>O and CO<sub>2</sub> using room-temperature ionic liquid [bmim][Ac]. *Sep Sci Technol.* 2012;47:411–421.
124. Zeng SJ, Zhang X, Bai LP, Zhang XC, Wang H, Wang JJ, Bao D, Li MD, Liu XY, Zhang SJ. Ionic-liquid-based CO<sub>2</sub> capture systems: structure, interaction and process. *Chem Rev.* 2017;117:9625–9673.
125. Liu XY, He MG, Lv N, Xu HD, Bai LH. Selective absorption of CO<sub>2</sub> from H<sub>2</sub>, O<sub>2</sub> and N<sub>2</sub> by 1-hexyl-3-methylimidazolium tris(pentafluoroethyl)trifluorophosphate. *J Chem Thermodyn.* 2016;97:48–54.
126. Finotello A, Bara JE, Narayan S, Camper D, Noble RD. *J Phys Chem B.* 2008;112:2335–2339.
127. Nicola GD, Giuliani G, Polonara F. Isochoric PVT<sub>x</sub> measurements for the CO<sub>2</sub> + N<sub>2</sub>O system. *J Chem Eng Data.* 2005;50:656–660.
128. Peng X, Wang W, Xue R, Shen Z. Adsorption separation of CH<sub>4</sub>/CO<sub>2</sub> on mesocarbon microbeads: experiment and modeling. *AIChE J.* 2006;52:994–1003.
129. Pérez-Ramírez J, Kapteijn J, Schöffel K, Moulijn JA. Formation and control of N<sub>2</sub>O in nitric acid production. Where do we stand today? *Appl Catal B Environ.* 2003;44:117–151.
130. Karelson M, Lobanov V, Katritzky AR. Quantum chemical descriptors in QSAR/QSPR studies. *Chem Rev.* 1996;96:1027–1044.
131. Eike DM, Brennecke JF, Maginn EJ. Predicting infinite-dilution activity coefficients of organic solutes in ionic liquids. *Ind Eng Chem Res.* 2004;43:1039–1048.
132. Tämm K, Burk P. QSPR analysis for infinite dilution activity coefficients of organic compounds. *J Mol Model.* 2006;12:417–421.
133. Katritzky AR, Kuanar M, Stoyanova-Slavova IB, Slavov SH, Dobchev DA, Karelson M, Acree WE, Jr. Quantitative structure–property relationship studies on

- Ostwald solubility and partition coefficients of organic solutes in ionic liquids. *J Chem Eng Data*. 2008;53:1085–1092.
134. Ghaslani D, Gorji ZE, Gorji AE, Riahi S. Descriptive and predictive models for Henry's law constant of CO<sub>2</sub> in ionic liquids: a QSPR study. *Chem Eng Res Des*. 2017;120:15–25.
  135. Mehraein I, Riahi S. The QSPR models to predict the solubility of CO<sub>2</sub> in ionic liquids based on least-squares support vector machines and genetic algorithm-multilinear regression. *J Mol Liq*. 2017;225:521–530.
  136. Zhao Y, Gao J, Huang Y, Afzal RH, Zhang X, Zhang S. Predicting H<sub>2</sub>S solubility in ionic liquids by the quantitative structure–property relationship method using S<sub>σ-profile</sub> molecular descriptors. *RSC Adv*. 2016;6:70405
  137. Abraham MH. Scales of solute hydrogen-bonding: their construction and application to physicochemical and biochemical processes. *Chem Soc Rev*. 1993;22:73–83.
  138. Mintz C, Acree W. Partition coefficient correlations for transfer of solutes from gas phase and water to room temperature ionic liquids. *Phys Chem Liq*. 2007;45:241–249.
  139. Sprunger L, Clark M, Acree WE, Jr., Abraham MH. Characterization of room-temperature ionic liquids by the Abraham model with cation-specific and anion-specific equation coefficients. *J Chem Inf Model*. 2007;47:1123–1129.
  140. Nami F, Deyhimi F. Prediction of activity coefficients at infinite dilution for organic solutes in ionic liquids by artificial neural network. *J Chem Thermodyn*. 2011;43:22–27.
  141. Faundez CA, Fierro EN, Valderrama JO. Solubility of hydrogen sulfide in ionic liquids for gas removal processes using artificial neural networks. *J Environ Chem Eng*. 2016;4:211–218.
  142. Eslamimanesh A, Gharagheizi F, Mohammadi AH, Richon D. Artificial neural network modeling of solubility of supercritical carbon dioxide in 24 commonly used ionic liquids. *Chem Eng Sci*. 2011;66:3039–3044.
  143. Oliferenko AA, Oliferenko PV, Seddon KR, Torrecilla JS. Prediction of gas solubilities in ionic liquids. *Phys Chem Chem Phys*. 2011;13:17262–17272.
  144. Padaszyński K. In silico calculation of infinite dilution activity coefficients of molecular solutes in ionic liquids: critical review of current methods and new models based on three machine learning algorithms. *J Chem Inf Model*. 2016;56:1420–1437.
  145. Zheng YZ, Wang NN, Luo JJ, Zhou Y, Yu ZW. Hydrogen-bonding interactions between [BMIM][BF<sub>4</sub>] and acetonitrile. *Phys Chem Chem Phys*. 2013;15:18055–18064.
  146. Bernales VS, Marenich AV, Contreras R, Cramer CJ, Truhlar DG. Quantum mechanical continuum solvation models for ionic liquids. *J Phys Chem B*. 2012;116:9122–9129.
  147. Diedenhofen M, Eckert F, Klamt A. Prediction of infinite dilution activity coefficients of organic compounds in ionic liquids using COSMO-RS. *J Chem Eng Data*. 2003;48:475–479.
  148. Diedenhofen M, Klamt A. COSMO-RS as a tool for property prediction of IL mixtures—a review. *Fluid Phase Equilib*. 2010;294:31–38.
  149. Gutiérrez JP, Meindersma GW, de Haan AB. COSMO-RS-based ionic liquid selection for extractive distillation processes. *Ind Eng Chem Res*. 2012;51:11518–11529.
  150. Lei Z, Arlt W, Wasserscheid P. Separation of 1-hexene and n-hexane with ionic liquids. *Fluid Phase Equilib*. 2006;241:290–299.
  151. Mohanty S, Banerjee T, Mohanty K. Quantum chemical based screening of ionic liquids for the extraction of phenol from aqueous solution. *Ind Eng Chem Res*. 2010;49:2916–2925.
  152. Ab Manan N, Hardacre C, Jacquemin J, Rooney DW, Youngs TGA. Evaluation of gas solubility prediction in ionic liquids using COSMOthermX. *J Chem Eng Data*. 2009;54:2005–2022.
  153. Lin ST, Sandler SI. *A priori phase equilibrium prediction from a segment contribution solvation model*. *Ind Eng Chem Res*. 2002;41:899–913.
  154. Lee BS, Lin ST. Screening of ionic liquids for CO<sub>2</sub> capture using the COSMO-SAC model. *Chem Eng Sci*. 2015;121:157–168.
  155. Padaszyński K. An overview of the performance of the COSMO-RS approach in predicting the activity coefficients of molecular solutes in ionic liquids and derived properties at infinite dilution. *Phys Chem Chem Phys*. 2017;19:11835–11850.
  156. Hanke CG, Atamas NA, Lynden-Bell RM. Solvation of small molecules in imidazolium ionic liquids. A simulation study. *Green Chem*. 2002;4:107–111.
  157. Lynden-Bell RM, Atamas NA, Vasilyuk A, Hanke CG. Chemical potentials of water and organic solutes in imidazolium ionic liquids: a simulation study. *Molec Phys*. 2002;100:3225–3229.
  158. Deschamps J, Costa Gomes M, Padua AAH. Molecular simulation study of interactions of carbon dioxide and water with ionic liquids. *Chem Phys Chem*. 2004;5:1049–1052.
  159. Shah JK, Maginn EJ. A Monte Carlo simulation study of the ionic liquid 1-n-butyl-3-methylimidazolium hexafluorophosphate: liquid structure, volumetric properties and infinite dilution solution thermodynamics with CO<sub>2</sub>. *Fluid Phase Equilib*. 2004;222–223:195–203.
  160. Shi W, Thompson RL, Albenze E, Steckel JA, Nulwala HB, Luebke DR. Contribution of the acetate anion to CO<sub>2</sub> solubility in ionic liquids: theoretical method development and experimental study. *J Phys Chem B*. 2014;118:7383–7394.
  161. Urukova I, Vorholz J, Maurer G. Solubility of CO<sub>2</sub>, CO and H<sub>2</sub> in the ionic liquid [bmim][PF<sub>6</sub>] from Monte Carlo simulations. *J Phys Chem B*. 2005;109:12154–12159.
  162. Urukova I, Vorholz J, Maurer G. Correction to “Solubility of CO<sub>2</sub>, CO and H<sub>2</sub> in the ionic liquid [bmim][PF<sub>6</sub>] from Monte Carlo simulations.” *J Phys Chem B*. 2006;110:18072–18072.
  163. Shi W, Maginn EJ. Atomistic simulation of the absorption of carbon dioxide and water in the ionic liquid 1-n-hexyl-3-methylimidazolium bis(trifluoromethylsulfonyl)imide ([hmim][Tf<sub>2</sub>N]). *J Phys Chem B*. 2008;112:2045–2055.
  164. Zhang X, Huo F, Liu Z, Wang W, Maginn E, Shi W. Absorption of CO<sub>2</sub> in the ionic liquid 1-n-hexyl-3-

- methylimidazolium tris(pentafluoroethyl)trifluorophosphate ([hmim][FEP]): a molecular view by computer simulations. *J Phys Chem B*. 2009;113:7591–7598.
165. Kerlé D, Ludwig R, Geiger A, Paschek D. Temperature dependence of the solubility of carbon dioxide in imidazolium-based ionic liquids. *J Phys Chem B*. 2009;113:12727–12735.
  166. Shi W, Maginn EJ. Molecular simulation of ammonia absorption in the ionic liquid 1-ethyl-3-methylimidazolium bis(trifluoromethylsulfonyl)imide ([emim][Tf<sub>2</sub>N]). *AIChE J*. 2009;55:2414–2421.
  167. Jamali SH, Ramdin M, Becker TM, Torres-Knoop A, Dubbeldam D, Buijs W, Vlught YJH. Solubility of sulfur compounds in commercial physical solvents and an ionic liquid from Monte Carlo simulations. *Fluid Phase Equilib*. 2017;433:50–55.
  168. Ramdin M, Chen Q, Balaji SP, Vicent-Luna JM, Torres-Knoop A, Dubbeldam D, Calero S, de Loos TW, Vlught TJH. Solubilities of CO<sub>2</sub>, CH<sub>4</sub>, C<sub>2</sub>H<sub>6</sub>, and SO<sub>2</sub> in ionic liquids and selexol from Monte Carlo simulations. *J Comput Sci*. 2016;15:74–80.
  169. Marin-Rimoldi E, Shah JK, Maginn EJ. Monte Carlo simulations of water solubility in ionic liquids: a force field assessment. *Fluid Phase Equilib*. 2016;407:117–125.
  170. Budhathoki S, Shah JK, Maginn EJ. Molecular simulation study of the performance of supported ionic liquid phase materials for the separation of carbon dioxide from methane and hydrogen. *Ind Eng Chem Res*. 2017;56:6775–6784.
  171. Sambasivarao SV, Acevedo O. Development of OPLS-AA force field parameters for 68 unique ionic liquids. *J Chem Theory Comput*. 2009;5:1038–1050.
  172. Canongia Lopes JN, Pádua AAH. CL&P: a generic and systematic force field for ionic liquids modeling. *Theor Chem Acc*. 2012;131:1129–1139.
  173. Bates ED, Mayton RD, Ntai I, Davis JH. CO<sub>2</sub> capture by a task-specific ionic liquid. *J Am Chem Soc*. 2002;124:926–927.
  174. Menjoge A, Dixon J, Brennecke JF, Maginn EJ, Vasenkov S. Influence of water on diffusion in imidazolium-based ionic liquids: a pulsed field gradient NMR study. *J Phys Chem B*. 2009;113:6353–6359.
  175. Hazelbaker ED, Budhathoki S, Katihar A, Shah JK, Maginn EJ, Vasenkov S. Combined application of high-field diffusion NMR and molecular dynamics simulations to study dynamics in a mixture of carbon dioxide and an imidazolium-based ionic liquid. *J Phys Chem B*. 2012;116:9141–9151.
  176. He M, Peng S, Liu X, Pan P, He Y. Diffusion coefficients and Henry's constants of hydrofluorocarbons in [HMIM][Tf<sub>2</sub>N], [HMIM][TFO], and [HMIM][BF<sub>4</sub>]. *J Chem Thermodyn*. 2017;112:43–51.
  177. Almantariotis D, Fandiño O, Coxam J-Y, Costa Gomes MF. Direct measurement of the heat of solution and solubility of carbon dioxide in 1-hexyl-3-methylimidazolium bis(trifluoromethylsulfonyl)amide and 1-octyl-3-methylimidazolium bis(trifluoromethylsulfonyl)amide. *Int J Greenhouse Gas Control*. 2012;10:329–340.
  178. Broderick A, Khalifa Y, Shiflett MB, Newberg JT. Water at the ionic liquid-gas interface examined by ambient pressure x-ray photoelectron spectroscopy. *J Phys Chem C*. 2017;121:7337–7343.
  179. Zhang B, van Duin ACT, Johnson JK. Development of a ReacFF reactive force field for tetrabutylphosphonium glycinate/CO<sub>2</sub> mixtures. *J Phys Chem B*. 2014;118:12008–12016.
  180. Balaji SP, Gangarapu S, Ramdin M, Torres-Knoop A, Zuilhof H, Goetheer ELV, Dubbeldam D, Vlught TJH. Simulating the reaction of CO<sub>2</sub> in aqueous monoethanolamine solution by reaction ensemble Monte Carlo using the continuous fractional component method. *J Chem Theory Comput*. 2015;11:2661–2669.
  181. Firaha DS, Holloczki O, Kirchner B. Computer-aided design of ionic liquids as CO<sub>2</sub> absorbents. *Angew Chem Int Ed Engl*. 2015;54:7805–7809.
  182. Gebicki J, Kloskowski A, Chrzanowski W, Stepnowski P, Namiesnik J. Application of ionic liquids in amperometric gas sensors. *Crit Rev Anal Chem*. 2016;46(2):122–138.
  183. Behera K, Pandey S, Kadyan A, Pandey S. Ionic liquid-based optical and electrochemical carbon dioxide sensors. *Sensors*. 2015;15:30487–30503.
  184. Cowan MG, Gin DL, Noble RD. Poly(ionic liquid)/ionic liquid ion-gels with high “free” ionic liquid content: platform membrane materials for CO<sub>2</sub>/light gas separations. *Acc Chem Res*. 2016;49:724–732.
  185. Tomé LC, Marrucho IM. Ionic liquid-based materials: a platform to design engineered CO<sub>2</sub> separation membranes. *Chem Soc Rev*. 2016;45:2785–2824.
  186. Karkhanechi H, Salmani S, Asghari M. A review on gas separation applications of supported ionic liquid membranes. *ChemBioEng Rev*. 2015;2(4):290–302.
  187. Makino T, Kanakubo M. CO<sub>2</sub> absorption property of ionic liquid and CO<sub>2</sub> permselectivity for ionic liquid membrane. *J Jpn Petrol Inst*. 2016;59(4):109–117.
  188. Cui G, Wang J, Zhang S. Active chemisorption sites in functionalized ionic liquids for carbon capture. *Chem Soc Rev*. 2016;45:4307–4339.
  189. Theo WL, Lim JS, Hashim H, Mustaffa AA, Ho WS. Review of pre-combustion capture and ionic liquid in carbon capture and storage. *Appl Energy*. 2016;183:1633–1663.
  190. Babamohammadi S, Shamiri A, Aroua MK. A review of CO<sub>2</sub> capture by absorption of ionic liquid-based solvents. *Rev Chem Eng*. 2015;31(4):383–412.
  191. Öchsner E, Schneider MJ, Meyer C, Haumann M, Wasserscheid P. Challenging the scope of continuous, gas-phase reactions with supported ionic liquid phase (SILP) catalysts—asymmetric hydrogenation of methyl acetoacetate. *Appl Catal A Gen*. 2011;399:35–41.
  192. Joni J, Haumann M, Wasserscheid P. Continuous gas-phase isopropylation of toluene and cumene using highly acidic Supported Ionic Liquid Phase (SILP) catalysts. *Appl Catal A Gen*. 2010;372:8–15.
  193. Werner S, Szesni N, Bittermann A, Schneider MJ, Härter P, Haumann M, Wasserscheid P. Screening of Supported Ionic Liquid Phase (SILP) catalysts for the very low temperature water—as-shift reaction. *Appl Catal A Gen*. 2010;377:70–75.
  194. Riisager A, Jorgensen B, Wasserscheid P, Fehrmann R. First application of supported ionic liquid phase (SILP)

- catalysis for continuous methanol carbonylation. *Chem Commun.* 2006;9:994–996.
195. Zheng Y, Wang C, Armstrong DW, Woods RM, Jayawardhana DA. Rapid, efficient quantification of water in solvents and solvents in water using an ionic liquid-based GC column. *LCGC.* 2012;30(2):142–158.
196. Sigma-Aldrich ionic liquid gas chromatography columns. Available from <http://www.sigmaaldrich.com/analytical-chromatography/analytical-products.html>.
197. Queen's University Ionic Liquids Laboratory (QUILL). Available from <http://www.qub.ac.uk/schools/SchoolofChemistryandChemicalEngineering/Research/ResearchCentres/>.
198. Mahpuzah A, Atkins MP, Hassan A, Holbrey JD, Kuah Y, Nockemann P, Olfierenko AA, Plechkova NV, Rafeen S, Rahman AA, Ramli R, Shariff SM, Seddon KR, Srinivasan G, Zou Y. An ionic liquid process for mercury removal from natural gas. *Dalton Trans.* 2015; 44:8617–8624.
199. McCoy M. Chevron embraces ionic liquids. *Chem Eng News.* 2016;94(39):16.
200. Timken HKC, Elomari S, Trumbull S, Cleverdon R. Integrated alkylation process using ionic liquid catalysts. US Patent 7,432,408 Oct. 7, 2008.
201. Elomari S, Trumbull S, Timken HKC, Cleverdon R. Alkylation process using chloroaluminate ionic liquid catalysts. US Patent 7,432,409 Oct. 7, 2008.
202. Shiflett MB, Scurto AM. *Ionic Liquids: Current State and Future Directions.* ACS Publications, 2017.

